Natural and pathological aging distinctively impact the vomeronasal system and social behavior

Adrián Portalés[1], Pablo Chamero[2], Sandra Jurado[1]*

Author affiliation:

[1]Institute of Neuroscience CSIC-UMH, San Juan de Alicante, Alicante, Spain
[2] Laboratoire de Physiologie de la Reproduction et des Comportements, CNRS, IFCE, INRAE, University of Tours, 37380, Nouzilly, France
*Corresponding author: Sandra Jurado (sjurado@umh.es)

Keywords: Aging, pheromone, vomeronasal system, social behavior, odor discrimination, neurodegeneration

Abstract

Normal aging and many age-related disorders such as Alzheimer´s disease cause deficits in olfaction, however it is currently unknown how natural and pathological aging impact the detection of social odors which might contribute to the impoverishment of social behavior at old age further worsening overall health. Here, we investigated the effect of aging in the recognition of social cues and the display of social behavior. Our findings indicate that aging distinctively disrupts the processing of social olfactory cues decreasing social odor exploration, discrimination and habituation in both wild type senescent (2-year-old) mice and in 1-year-old double mutant model of Alzheimer´s disease (APP/PS1^{Het}). Furthermore, social novelty was diminished in 1-year-old APP/PS1 mice, indicating that alterations in the processing of social cues are accelerated during pathological aging. Analysis of the vomeronasal organ, the main gateway to pheromone-encoded information, indicated that natural and pathological aging distinctively reduce the neurogenic ability of the vomeronasal sensory epithelium. Cell proliferation remained majorly preserved in 1-year model of Alzheimer´s disease (APP/PS1^{Het}), whereas naturally aged animals exhibited significant deficiencies in the number of mature, proliferative and progenitor cells. This study reveals fundamental differences in the cellular processes by which natural and pathological aging disrupt the exploration of social cues and social behavior.

Introduction

Social recognition is essential for survival allowing to appropriately adapt behavior across a variety of contexts (Adolphs, 2001; Brennan and Kendrick, 2006). As aging progresses, social odors have been shown to elicit attenuated responses (Hlinák and Krejcí, 1991; Garrat et al., 2011), a phenomenon interpreted as a natural consequence of age-related decline in sensory perception (Doty et al., 1984; Murphy et al., 2002; Doty and Kamath, 2014), that might negatively impact the social behavior of aged animals, whose survival might become increasingly dependent on the social environment. In humans, social impoverishment has been identified as a major aggravating factor for decreased life expectancy, and an indicator of the appearance of dementia and neurodegenerative disorders such as Alzheimer´s disease (AD) (Wilson et al., 2007; Heinrichs et al., 2003; Donovan et al., 2016). Despite the central role of social interaction in maintaining overall well-being, the mechanisms by which aging, natural or pathological, alter social information processing remain unclear.

Mouse social communication strongly depends on chemosignals comprised by a heterogeneous mix of volatile and non-volatile molecules (pheromones) (Petrulis and Johnston, 1997; Beynon and Hurst, 2004; Yoon et al., 2005; Baum and Kelliher, 2009; Chamero et al., 2012; Noack et al., 2010; Tobin et al., 2010; Li and Dulac, 2018). Volatile odors are primarily detected at the main olfactory epithelium (MOE) which projects to the main olfactory bulb (MOB), whereas pheromones are mainly detected by

the vomeronasal sensory epithelium (VSE) (Jacobson, 1813; Halpern and Martinez-Marcos, 2003; Munger et al., 2009) which connects to the accessory olfactory bulb (AOB) (Shipley et al., 2008). However, both systems have overlapping and complementary functions in relation to the stimuli they are able to detect and the behavioral or physiological output they can generate (Brennan and Zufall, 2006; Zufall and Leinders -Zufall, 2007).

A remarkable property of the VSE is that contains proliferative niches capable of generating new cells majorly becoming functional neurons during adulthood (Weiler, 2005; Weiler et al., 1999; Whitman and Greer, 2009; Graziadei and Monti Graziadei, 1983; Halpern and Martínez-Marcos, 2003; Brann and Firestein, 2014; De la Rosa-Prieto et al., 2009; Oboti et al., 2015). The neurogenic properties of olfactory structures are known to decline with age (Bailey et al., 2004; Ahlenius et al., 2009; Wagner et al., 2009), a phenomenon proposed to underlie the olfactory deficits associated to both natural aging and neurodegenerative disorders (Doty et al., 1984; Murphy et al., 2002; Doty and Kamath, 2014; Devanand, 2016; Mobley et al., 2014; Lazarov and Marr, 2010). However, how natural and pathological aging affect the regenerative capacity of the VSE has been scarcely studied despite being central to socio-sexual cue detection. Previous studies have shed some light into VSE anatomical alterations induced by natural aging. An elegant study by Brann and Firestein (2010) showed that the proliferative capacity of the VSE of 2-year-old animals was attenuated in comparison to young animals. More recently, Mechin et al., (2021) explored the effects of natural aging on VSE cell proliferation, finding a significant reduction in mature Olfactory Marker Protein (OMP)-expressing cells (OMP^+), indicating structural modifications of the aged VNO. However, whether these alterations in the aged VSE have any impact in odor detection and subsequent display of social behaviors, particularly in animal models of neurodegeneration, is currently unclear.

To gain insight into these questions, we investigated the impact of natural and pathological aging in social odor-evoked sniffing behavior, social-odor habituation/dishabituation and social behavior during the aging process of wild type C57/BL6 mice and amyloid precursor protein (APP) and presinilin-1 (PS1) (APPswe/PS1ΔE9) double transgenic mice ($APP/PS1^{Het}$ mice, therein), a widely used animal model of AD (Jankowsky et al., 2001; Jankowsky et al., 2004). Analysis of the number of progenitors, proliferative and mature neurons revealed that naturally aged animals show reduced neuronal proliferation and decreased levels of sensory mature (OMP^+) neurons. In contrast, the VSE of middle age (1-year-old) $APP/PS1^{Het}$ mice exhibited normal levels of mature neurons and cell regeneration, suggesting that natural and pathological aging distinctively impact the neurogenic capacity of the VSE.

We explored the functional consequences of these cellular alterations observing reduced exploration time of social odors and decreased performance in a social odor habituation-dishabituation test in both senescent and middle age $APP/PS1^{Het}$ mice, suggesting that despite the overall normal VSE structure and cell composition, $APP/PS1^{Het}$ animals exhibit an accelerated decay of the processing of social cues. Moreover, 1-year-old APP/PS^{Het} mice exhibited a significant reduction of social novelty which was no apparent in naturally aged animals, exposing a fundamental difference in how natural and pathological aging impact the regulation of social behavior.

Materials and Methods

Animals

Experiments were performed in either control C57/BL6 mice (young: 2-4 months-old; adult: 6-8 months-old; middle age: 12-14 months-old; old (senescent): 20-24 months-old) or APP/PS1 on a C57/BL6 genetic background (young: 2-4 months-old; middle-age: 12-14 months-old) (Jackson Labs, Stock No. 004462, MMRRC Stock No. 34829). $APP/PS1^{Het}$ mice express a chimeric mouse/human amyloid precursor protein (Mo/HuAPP695swe) and a mutant human presenilin 1 (PS1-dE9). These animals develop beta-amyloid deposits at ~ 6 - 7 months of age and exhibit early-onset cognitive impairments (Jankowsky et al., 2001, 2004; Reiserer et al., 2007). Animals were kept group-housed and

experimentally-naïve during all their lifetime under pathogen-free conditions. Animals were housed in ventilated cages with free access to food and water on a 12 h light/dark cycle.

All experiments were performed according to Spanish and European Union regulations regarding animal research (2010/63/EU), and the experimental procedures were approved by the Bioethical Committee at the Instituto de Neurociencias and the Consejo Superior de Investigaciones Científicas (CSIC).

VNO dissection

Mice were perfused transcardially with PBS, pH 7.4, followed by 4% paraformaldehyde in 0.1 M phosphate buffer (PB), pH 7.4. A fixed mouse head was placed under a scope and the lower jaw was removed to get a palate view. To facilitate VNO extraction, the palate and the nasal septum were removed and the bilateral VNOs were split in two parts with a gentle twisting motion. Finally, the cartilaginous tissue that covers each portion was carefully removed to extract the VNOs. Tissue was incubated in a 30 % sucrose solution for cryoprotection and kept at -4 ºC until sectioning. Samples were embedded in OCT and frozen at -80 ºC for cryosectioning.

Immunohistochemistry

VNOs embedded in OCT were sliced in 16 μm thick sections in a cryostat apparatus (Leica CM 3050S). Slices were incubated in blocking solution containing 0.5 % Triton X-100 and 5 % normal horse serum in 0.1 M TBS for 2 h at room temperature (RT). Primary antibody incubation was performed overnight (o/n) at 4 ºC against OMP (Wako goat polyclonal; 1:2000), PCNA (Sigma, rabbit monoclonal; 1:2000); Sox2 (R&D Systems, goat polyclonal; 1:300). For PCNA immunostaining, slices were incubated in 10 mM citrate buffer (100 ºC; pH, 6) for 5 minutes prior staining. Sections were incubated with Alexa Fluor 488- or 594- conjugated secondary antibodies (Jackson Laboratories, 1:500) for 2 h at RT. Hoechst (Sigma, 1:10000) was added during 5 minutes after the secondary antibody incubation for nuclei visualization. Imaging was performed using a vertical confocal Microscope Leica SPEII. Final images were assembled with Adobe Illustrator.

Sox2 fluorescence intensity at the VNO supporting cell layer

For determining the Sox2 fluorescent labeling area in the VNO supporting cell layer (SCL) where single-cell quantification was limited by the densely packed disposition of the cells, we calculated the corrected total fluorescence (CTF) of the area of interest employing the Freehand ROI tool of Image J. CTF was calculated by subtracting the background fluorescence from a minimum of 3 sections, 16 μm thick from at least 4 animals per condition.

Stereology, cell quantification and AOB volume estimation

The total number of olfactory mature neurons (OMP^+ neurons) in the entire VSE was estimated using the optical fractionator method (Wong et al., 2018) included in the Stereo Investigator software (MBF Bioscience). Two different tools are combined in this unbiased quantification method: a 3D optical dissector for cell counting and a fractionator, which is based on a systematic, uniform and random sampling over a known area of the tissue (West and Gundersen, 1990; Dorph-Petersen and Lewis, 2011; Parrish-Aungst et al., 2007). The number of neurons is estimated as:

$$N = (1/h \times 1/ssf \times 1/asf) \times \sum Q - t$$

In which $\sum \mathbf{Q}$ is the total cell number in the region of interest acquired using the optical dissector method; **t** stands for the mean mounted section thickness; **h** is the optical dissector height; **asf** is the area sampling fraction and **ssf** is the frequency of sampling (section sampling fraction). For the VSE stereological analysis, sampling was performed with a 20x objective (Leica, NA 0.6), the counting frame area was 2500 μm^2 and the sampling grid area was 22500 μm^2; h for VSE stereology was 8 μm

with 1 μm as upper and lower guard zones and t was set at 10 μm. Quantifications were performed for the central, intermediate and marginal regions of the VSE dividing the area in segments of equal length as previously described (Giacobini et al., 2000; Brann and Firestein, 2010). For the cell quantification in the anterior-posterior regions, the VSE was divided in 10 sections per animal and the results were divided by the area to obtain the number of cells/mm^2 in each subdivision. Quantification of the number of cells in the marginal and central areas was performed in three slices of each animal delineated with a 50x50 dissector employing Stereo Investigator (MBF Bioscience).

VSE volume was calculated by multiplying the sampled area by the slice thickness (16 μm) and the number of series (10 slices per animal). Ten sections per series were analyzed to obtain an estimation of the VSE area and volume in young (4 months-old), aged (24 months-old), middle aged (12-months old) APP/$PS1^{WT}$ and middle aged APP/$PS1^{Het}$ mice.

The volume of the AOB was estimated by measuring the AOB area and multiplying the sampled area by the section thickness (50 μm) and the number of analyzed sections (5 series per animal).

Odorants

Social and non-social scents were employed to discern the impact of aging in social odor perception. As non-social scents, we used **i)** the banana-like odor isoamyl acetate (Sigma) shown to be primarily detected at the MOE level (Xu et al., 2005) with neutral valence within a broad dilution range (Fortés-Marco et al., 2015; Root et al., 2014; Saraiva et al., 2016), and **ii)** food pellets to perform a food finding test (FFT, see experimental details below). As a social scent, we used mouse urine as urine from conspecifics has been shown to elicit robust VNO activity (Chamero et al., 2017). Urine samples were collected according to standard procedures (Kurien et al., 2004). For habituation-dishabituation tests, frozen urine samples from different young subjects and cage mates were used to test fine odor discrimination. For sensitivity tests, urine samples were combined in a stock sample used for each round of odor presentations until completing the experiments. For female urine, samples obtained at different points of the estrous cycle were pooled to generate a uniform stock.

Behavioral assessment

All the behavioral experiments using social and non-social stimuli were performed in a dedicated room with continuous air reposition under dim indirect light (20 lx). Odor dilutions were prepared in a room outside the animal house. Odor presentation was performed in a homemade methacrylate box with removable walls for cleaning. The chamber dimensions were 15 cm width, 15 cm length and 30 cm high. A small hole (1cm diameter) was performed in the middle of one of the sides located 5 cm above from the box ground to fit standard cotton sticks impregnated with 1 μL of the odorant (**Figure 3A**) allowing direct contact with the stick. Habituation to the testing conditions was performed before odorant presentations consisting of: handling (5 min), free exploratory activity in the box and habituation to the cotton stick movement (5 min). Odors were presented embedded in a cotton stick in order to preserve non-volatile pheromones and mimic the natural detection method of physical contact between conspecifics (Leypold et al., 2002; Stowers et al., 2002; Kimchi et al., 2007). To avoid variability due to the intensity of the volatile components of the urine, only direct nose contact with the tip of the cotton stick were considered as explorative behavior (sniffing/exploration time). Experiments were monitored by a video recording camera fixed 15 cm above the box. Videos were collected and analyzed off-line using SMART video-tracking software (PanLab S.L.).

a) *Odor exploration test*: After a period of habituation (10 min), mice were exposed to two control trials (mineral oil for isoamyl acetate assays or water for urine tests) during 1 min separated by intervals of 1 min to avoid lack of novelty and odor habituation (Breton-Provencher et al., 2009; Sanderson and Bannerman, 2011). Subsequent presentations consisted on serial dilutions of either urine samples (diluted in water: 1:1.000, 1:500, 1:250, 1:100, 1:50, 1:10 and non-diluted, nd) or isoamyl-acetate were

tested in ascending order (diluted in mineral oil: 1:5x10^5, 1:100.000, 1:10.000; 1:1.000, 1:100). Animals were considered to detect the olfactory stimulus when spent more time investigating the odors than the vehicles (water or mineral oil).

b) *Food finding test (FFT)*: Food finding test (FFT) was performed following standard procedures (Deacon et al., 2009). The mice were food deprived for 24 h before testing. Five food pellets (~ 35 g) were placed a corner and covered by 5 cm of litter bedding. Animals were considered to detect the food pellet when spent digging, touching and holding the food pellet for more than 5 s.

c) *Social odor habituation-dishabituation test:* The effect of aging in social odor discrimination and habituation was explored using an adapted habituation-dishabituation test (Gheusi et al., 2000). After a period of cage habituation (10 min), two control trials were performed employing cotton sticks soaked with 1μl of water (vehicle). Three successive presentations of urine from an animal of the opposite sex (S1a-c) were followed by three presentations of urine from a different subject of the opposite-sex (S2a-c) to evaluate fine chemo-olfactory discrimination and habituation. Urine samples came from young animals of the opposite sex to maximize approaching behavior (Xu et al., 2005; Garratt et al., 2011). Each sample presentation lasted 1 min separated by 1 min intervals. Habituation was estimated as a decrease in the exploration time (sniffing) over the cotton stick tip after the first exposure of urine from the same animal (S1a). Dishabituation (discrimination) occurs in response to a new odor presentation (S2a) as a measurable increase in the exploration time. The test allows to explore two consecutive phases of discrimination (H_2O^B-S1a and S1c-S2a) and habituation (S1a-S1b and S2a-S2b). Trend lines between H_2O^B-S1a, S1c-S2a, S1a-S1b and S2a-S2b were fitted to obtain the slope values indicating the amplitude of the discrimination and habituation effect in each tested condition. Higher positive values indicated more pronounced social discrimination and higher negative values corresponded to more robust habituation (**Supplementary Figures 8 and 9**).

d) *Long-term social habituation-dishabituation test*: The aforementioned social odor habituation task was adapted to assay social cue memory by presenting the urine sample employed in S1a 24 hours after the first test was performed. Intact social odor memory manifested as a reduction in the sniffing time during the presentation of S1a during the second trial, an effect which was clearly apparent in young animals (**Figure 5F-G**).

e) *Three chamber test*: Social testing was performed in a cage (60 × 40 ×22 cm) following standard procedures (Nadler et al., 2004). Dividing walls were made from clear Plexiglas, with openings allowing access into each chamber. The test mouse was first placed in the middle chamber and allowed to explore for 10 minutes. After the habituation period, an unfamiliar subject of the same sex (mouse 1, M1), was placed in one of the side chambers. The stranger mouse was enclosed in a small, round wire cage, which allowed nose contact between the bars. In this first session (sociability), the test mouse had a choice of spending time in either the empty chamber (E) or the chamber occupied by M1. At the end of the sociability session, each mouse was tested in a second 10-minute session to evaluate social preference for a new subject. A second, unfamiliar mouse (mouse 2, M2) of the same sex was placed in the chamber that had been empty during the first session. This second stranger was enclosed in an identical wire cage than M1. The test mouse had a choice between the first, already-investigated mouse (M1), and the novel unfamiliar mouse (M2) which indicates their social preference or social novelty (Nadler et al., 2004). Continuous video recordings were collected and analyzed off-line using BORIS (Friard and Gamba, 2016) SMART video-tracking software (PanLab S.L.). Measures of time spent sniffing E, M1, and M2 were quantified for each session.

Statistical analysis

All data were tested for statistical significance using GraphPad Prism 8. Shapiro-Wilk test was used to determine data normality. One-way ANOVA with Tukey´s test for multiple comparisons with a single variable was implemented for cell quantifications and anatomical data. For the behavioral analysis, a

two-way ANOVA with Tukey´s test was used to test multiple comparisons with more than one variable. * $P \leq 0.05$; ** $P \leq 0.01$; *** $P \leq 0.001$.

Results

Structural modifications of the mouse VSE during natural and pathological aging

We sought to investigate the structure of the VSE during natural and pathological aging, as the main gateway of pheromone (non-volatile)-encoded information (Cheetham et al., 2007; Sharrow et al., 2002; Ferrero et al., 2013). Stereological analysis revealed significantly smaller VSE volumes in 2 year-old (senescent) mice (**Figure 1A**: VSE volume mm^3: 4 month-old: 0.190 ± 0.008; 1-year-old $APP/PS1^{WT}$: 0.170 ± 0.007; 24 month-old: 0.160 ± 0.007; 1-year-old $APP/PS1^{Het}$: 0.160 ± 0.008). This observation was supported by the reduced number of olfactory marker protein positive cells (OMP^+) along the anterior-posterior axis of the VSE and the analysis of the marginal (M), intermediate (I) and central (C) regions of the medial VSE (Halpern and Martinez-Marcos, 2003) in the VSE of 2-year old mice (**Supplementary Figure 1** and **Figure 1C, E**: number of OMP^+ cells $x10^3$ /μm^2: **Anterior**: 4 month-old: 10.69 ± 0.56; 12 month-old $APP/PS1^{WT}$: 9.50 ± 0.45; 24 month-old: 7.80 ± 0.53; 12 month-old $APP/PS1^{Het}$: 8.60 ± 0.53; **Medial**: 4 month-old: 9.92 ± 0.23; 12 month-old $APP/PS1^{WT}$: 9.15 ± 0.78; 24 month-old: 7.70 ± 0.70; 12 month-old $APP/PS1^{Het}$: 8.40 ± 0.40; **Posterior**: 4 month-old: 9.15 ± 0.70; 12 month-old $APP/PS1^{WT}$: 9.53 ± 0.77; 24 month-old: 7.90 ± 0.75; 12 month-old $APP/PS1^{Het}$: 10.00 ± 0.84).

We hypothesize that the drop in the number of OMP^+ cells could translate into a reduced axonal projection to the AOB, the main VNO target area, resulting in smaller AOB volumes. We observed reduced AOB size in 2 year-old mice (**Figure 1B:** AOB volume mm^3: 4 month-old: 0.48 ± 0.03; 12 month-old $APP/PS1^{WT}$: 0.48 ± 0.04; 24 month-old: 0.41 ± 0.03; 12 month-old $APP/PS1^{Het}$: 0.44 ± 0.03), indicating that aging alters basic structural features of the VNO-AOB axis.

We expanded our analysis to the SRY-box transcription factor 2 (Sox2)-expressing cells ($Sox2^+$) in the supporting cell layer (VSE SCL), a neuronal stem cell-marker which also stain mature differentiated sustentacular cells (Guo et al., 2010; Taroc et al., 2020; Katreddi et al., 2021). The estimation of the labeling intensity of Sox2 in the SCL showed a drastic reduction in senescent mice but not in $APP/PS1^{Het}$ mice (**Figure 1D, F**: Sox2 fluorescence intensity / area (μm^2): 4 month-old: 33.24 ± 2.43; 12 month-old: 26.23 ± 3.95; 24 month-old: 10.74 ± 1.32; 12 month-old $APP/PS1^{Het}$: 27.37 ± 0.96), indicating natural aging may disrupt the VSE structure by reducing the number of both sensory neurons and sustentacular cells (OMP^+ and $Sox2^+$).

Natural and pathological aging differentially impact cell proliferation in the VSE

The observed decrease in the number of mature OMP^+ and $Sox2^+$ cells in the VSE of senescent mice could be due to the reduction of the VSE´s regenerative ability. Furthermore, there is currently no available data on the status of the VSE neurogenic niche in neurodegenerative animal models. Thus, we analyzed the number of proliferative cells identified by the expression of proliferative cell nuclear antigen (PCNA) in the anterior, medial and posterior VNO. The marginal zone of the anterior and medial VSE proliferation was found more abundant consistently with previous reports (Giacobini et al., 2000; Brann and Firestein, 2010; **Figure 2A-B**). Senescent mice exhibited a significant reduction in $PCNA^+$ cells (**Figure 2A-B**, number of $PCNA^+$ cells x $10^3/mm^3$: **Anterior**: 4 month-old: 2.26 ± 0.80; 12 month-old $APP/PS1^{WT}$: 0.73 ± 0.3; 24 month-old: 0.75 ± 0.35; 12 month-old $APP/PS1^{Het}$: 3.42 ± 0.82; **Medial**: 4 month-old: 2.15 ± 0.52; 12 month-old $APP/PS1^{WT}$: 1.61 ± 0.32; 24 month-old: 0.23 ± 0.13; 12 month-old $APP/PS1^{Het}$: 1.57 ± 0.20; **Posterior**: 4 month-old: 3.04 ± 0.90; 12 month-old APP^{WT}: 2.42 ± 0.60; 24 month-old: 0.17± 0.08; 12 month-old $APP/PS1^{Het}$: 1.93 ± 0.57), indicating reduced proliferation. Surprisingly, the number of $PCNA^+$ cells in $APP/PS1^{Het}$ mice was significantly higher that of aged-matched controls in the anterior VNO (**Figure 2A-B**), suggesting an increased cell turnover in

these animals. Importantly, no significant overlap between OMP and PCNA staining was observed indicating that these two markers recognize cell populations at different maturation stages (**Supplementary Figure 2**).

We then sought to explore whether the reduced number of proliferative $PCNA^+$ cells in senescent mice could be due to a decrease of stem cell generation by analyzing the number of $Sox2^+$ neural precursor cells in the VSE (Tucker et al., 2010; Panaliappan et al., 2018). We observed a significant reduction in the number of $Sox2^+$ cells in 2 year-old mice but not in $APP/PS1^{Het}$ animals, indicating a reduced ability for progenitor generation in the aged VSE (**Figure 2C**: number of $Sox2^+$ cells in the VSE, number of cells x 10^4 cells/μm^2: 4 month-old: 3.08 ± 0.40; 12 month-old $APP/PS1^{WT}$: 2.92 ± 0.38; 24 month-old: 2.37 ± 0.36; 12 month-old $APP/PS1^{Het}$: 2.15 ± 0.24). Altogether, these findings revealed a fundamental difference in how natural and diseased aging impact the VSE structure and proliferative capacity.

Late onset of deficits in social exploration during natural aging

Our data indicated that natural aging induced significant alterations in the structure and proliferative ability of the VSE, thus we investigated whether these adaptations might translate into impairments in the processing of socio-sexual information. Cumulative evidence points to olfactory decline as a common symptom of natural and pathological aging (Doty et al., 1984; Murphy et al., 2002; Doty and Kamath, 2014; Rawson et al., 2012; Roberts et al., 2016). However, most of these studies and diagnostic tests employed synthetic odors with reduced emotional valence, therefore, the temporal course and severity of the age-related involution of the recognition of social cues, largely processed by the VNO-AOB system in the mouse, remains unclear.

To explore the impact of natural aging on social odor detection, we conducted an odor-evoked sniffing test in which serial dilutions of urine from young conspecifics of the opposite sex were presented to either male or female subjects over a range of different ages: young (2-4 mo.), adult (6-8 mo.), middle-aged (12-14 mo.) and old/senescent mice (20-24 mo.) (**Figure 3A**, see Material and Methods for details on urine sample preparation). Our results indicated a significant reduction in the exploration time throughout the various urine dilutions in comparison to adult wild type mice (**Figure 3B-C** sniffing time normalized to water control 2, **undiluted sample**: aged: 3.83 ± 0.71; adult: 6.06 ± 0.88; **1:10 dilution**: aged: 3.04 ± 0.50; adult: 4.90 ± 1.10; **1:50 dilution**: aged: 1.90 ± 0.33; adult: 3.14 ± 0.55; **1:100 dilution**: aged: 1.56 ± 0.37; adult: 2.95 ± 0.43; **1:250 dilution**: aged: 1.37 ± 0.36; adult: 2.36 ± 0.70; **1:500 dilution**: aged: 0.86 ± 0.20; adult: 2.50 ± 0.35; **1:1000 dilution**: aged: 0.60 ± 0.20; adult: 2.80 ± 0.43). Raw sniffing time data showed a similar decrease in the exploration of social odors in senescent animals across different dilutions (see details in **Supplementary Figures 3 and 4**).

Furthermore, senescent mice progressively increased the exploration time in parallel with odor concentration, whereas young, adult and middle-age animals showed a habituation phase at intermediate dilutions (1:500, 1:250, 1:100 and 1:50), indicating effective odor detection and recognition capabilities at low urine concentrations (Yang and Crawley, 2009). Data analysis disaggregated by sex showed that the reduction in exploration time was similar in male and female animals (**Supplementary Figure 5**; but see Martínez et al., 2017 for an alternative view).

Reduction in the exploration of social information is accelerated in an animal model of neurodegeneration

Next, we investigated whether pathological aging would affect the exploration of social olfactory cues despite no obvious effect on VSE structure or proliferative capacity. Social odor sensitivity tests in 1 year-old $APP/PS1^{Het}$ mice revealed reduced sniffing times when compared to age-matched $APP/PS1^{WT}$ control mice for low urine dilutions, suggesting that pathological aging accelerates the decline of exploration time of social odors (**Figure 3D-E** sniffing time normalized to water control 2, **undiluted sample**: 1 year-old $APP/PS1^{Het}$: 2.58 ± 0.43; 1 year-old $APP/PS1^{WT}$: 5.65 ± 1.51; **1:10 dilution**: 1 year-old $APP/PS1^{Het}$: 1.82 ± 0.27; 1 year-old $APP/PS1^{WT}$: 4.94 ± 1.21; **1:50 dilution**: 1 year-old $APP/PS1^{Het}$:

1.43 ± 0.46; 1 year-old APP/PS1^{WT}: 1.40 ± 0.26; **1:100 dilution**: 1 year-old APP/PS1^{Het}: 1.37 ± 0.43; 1 year-old APP/PS1^{WT}: 2.03 ± 0.55; **1:250 dilution**: 1 year-old APP/PS1^{Het}: 0.90 ± 0.17; 1 year-old APP/PS1^{WT}: 0.70 ± 0.14; **1:500 dilution**: 1 year-old APP/PS1^{Het}: 0.52 ± 0.10; 1 year-old APP/PS1^{WT}: 0.97 ± 0.20; **1:1000 dilution**: 1 year-old APP/PS1^{Het}: 1.00 ± 0.20; 1 year-old APP/PS1^{WT}: 0.84 ± 0.31). Similar to senescent mice, these results were reproduced when raw sniffing time data were compared (**Supplementary Figures 6 and 7**).

Aging and neurodegeneration impact social odor recognition more severely than other odor modalities

Next, we asked whether non-social odor modalities were also affected in senescent and APP/PS1^{Het} animals. We investigated this question by analyzing the exploration time to both food and synthetic neutral odors. First, we exposed naturally aged and APP/PS1^{Het} mice to serial dilutions of isoamyl acetate (IA), a synthetic banana like odor of neutral valence when used at high dilutions (Saraiva et al., 2016; Fortes-Marco, 2015). Consistent with previous studies, mice of all conditions showed significantly reduced responses to the neutral odorant than to urine (**Figure 4A-D**) according to the higher emotional valence of urine in comparison to a synthetic odor (Jagetia et al. 2018; Kobayakawa et al. 2007; Mandairon et al. 2009; Saraiva et al. 2016). Our results showed no significant differences on the exploration times of IA in senescent mice and a modest but significant increase in the sniffing time of the 1:10^4 and 1:100 IA dilutions in APP/PS1^{Het} animals (**Figures 4A-D,** normalized sniffing time, **1:100 dilution**: 1 year-old APP/PS1^{Het}: 1.40 ± 0.12; 1 year-old APP/PS1^{WT}: 0.93 ± 0.16; young: 1.76 ± 0.26; aged: 1.24 ± 0.20; 1:1000 dilution: 1 year-old APP/PS1^{Het}: 1.40 ± 0.22; 1 year-old APP/PS1^{WT}: 1.42 ± 0.30; young: 1.90 ± 0.35; aged: 1.56 ± 0.50; **1:10^4 dilution**: 1 year-old APP/PS1^{Het}: 1.50 ± 0.25; 1 year-old APP/PS1^{WT}: 0.91 ± 0.13; young: 1.44 ± 0.32; aged: 1.20 ± 0.26; **1:10^5 dilution**: 1 year-old APP/PS1^{Het}: 0.75 ± 0.11; 1 year-old APP/PS1^{WT}: 0.75 ± 0.15; young: 1.41 ± 0.50; aged: 0.90 ± 0.20; **1:5x10^5 dilution**: 1 year-old APP/PS1^{Het}: 0.85 ± 0.18; 1 year-old APP/PS1^{WT}: 0.82 ± 0.11; young: 1.65 ± 0.42; aged: 1.23 ± 0.35). Similarly, the food finding test showed no significant differences in the latency to find food pellets after 24 hours of food deprivation in either naturally aged or middle age APP/PS1^{Het} mice (**Figure 4E** latency of finding food pellet (min), young: 5.22 ± 1.08; aged: 5.15 ± 0.95; 1-year-old APP/PS1^{Het}: 4.27 ± 0.58; 1-year-old APP/PS1^{WT}: 3.87 ± 0.32). These results suggest that deficits in social exploration time at advanced stages of natural aging and in an animal model of AD are more pronounced than other odor modalities.

Social odor discrimination and habituation are reduced in naturally aged and APP/PS1^{Het} mice

To further investigate the impact of aging and neurodegeneration in the detection of social information, we performed a habituation – dishabituation test, which relies on the animal's ability to discriminate novel smells (Yang and Crawley, 2009). For these experiments, young (2-4 mo.) and aged (20-24 mo.) wild type animals were presented three consecutive replicates of urine samples from two different animals (S1a-c and S2a-c) (**Figure 5A**). Aged animals were able to discriminate between urine sources, but showed reduced sniffing times during both the first and second discrimination and habituation phases (**Figure 5B-C**). Similarly, middle age APP/PS1^{Het} mice also exhibited reduced sniffing times in comparison to aged-matched APP/PS1^{WT} controls (**Figures 5B-E** sniffing time in seconds, **water control 1**: aged: 0.56 ± 0.09; young: 0.42 ± 0.05; APP/PS1^{WT}: 0.72 ± 0.08; APP/PS1^{Het}: 0.57 ± 0.06; **water control 2**: aged: 0.56 ± 0.11; young: 0.67 ± 0.10; APP/PS1^{WT}: 0.50 ± 0.07; APP/PS1^{Het}: 0.71 ± 0.09; **S1a**: aged: 1.36 ± 0.27; young: 2.45 ± 0.40; APP/PS1^{WT}: 2.81 ± 0.40; APP/PS1^{Het}: 1.75 ± 0.22; **S1b**: aged: 0.70 ± 0.14; young: 0.87 ± 0.20; APP/PS1^{WT}: 0.95 ± 0.10; APP/PS1^{Het}: 0.68 ± 0.10; **S1c**: aged: 0.70 ± 0.21; young: 0.51 ± 0.10; APP/PS1^{WT}: 0.84 ± 0.22; APP/PS1^{Het}: 0.71 ± 0.13; **S2a**: aged: 1.51 ± 0.27; young: 2.44 ± 0.43; APP/PS1^{WT}: 1.85 ± 0.42; APP/PS1^{Het}: 1.00 ± 0.17; **S2b**: aged: 0.82 ± 0.14; young: 0.81 ± 0.15; APP/PS1^{WT}: 0.80 ± 0.22; APP/PS1^{Het}: 0.62 ± 0.08; **S2c**: aged: 0.96 ± 0.18; young: 0.55 ± 0.11); APP/PS1^{WT}: 0.60 ± 0.13; APP/PS1^{Het}: 0.50 ± 0.09). Analysis of the slope values of the first and second discrimination and habituation phases revealed that senescent mice exhibited

significant deficits during both rounds of social habituation – dishabituation, and APP/PS1^{Het} mice only during the second phase of discrimination (**Supplementary Figures 8 and 9**).

Then, we adapted the habituation-dishabituation test to assay potential changes in long-term social odor memory (**Figure 5F**). To this aim, animals were exposed to the same S1a urine sample 24 hours after the first presentation. A reduction of the sniffing time during the first discrimination phase was interpreted as an indicator of memory. This reduction was clearly observed in young animals, but absent in naturally aged and 1-year-old APP/PS1^{Het} mice (**Figure 5G:** sniffing time of S1a after 24 hours in seconds, young: 1.20 ± 0.20; aged: 1.12 ± 0.20; APP/PS1^{WT}: 1.40 ± 0.50; APP/PS1^{Het}: 1.20 ± 0.33), suggesting long-term social odor memory impairments during both natural and pathological aging.

Age-related deficits in social discrimination and habituation are not influenced by previous experience

Next, we compared animals exposed to either familiar (littermate urine, L) or novel social odors (novel urine, N) in the habituation-dishabituation test (**Figure 6A**). Aged animals performed poorly in the L-N dishabituation task (no significant increase in sniffing time), suggesting that the reduction in social odor discrimination and habituation is independent of previous experience.

Since impairments in social odor discrimination were more prominent in naturally aged mice, we asked whether these deficits also extended to the recognition of animal's own odors, as the loss of self-awareness is a disrupting symptom of common occurrence in senescent subjects (La Joie et al., 2016; Valech et al., 2018). To this aim, animals were presented to samples of their own urine (O) during the second discrimination phase of the habituation-dishabituation test (**Figure 6, C-D**). Our data indicated that animal´s own urine was effective to elicit a typical discrimination (dishabituation) response, (**Figure 6, C-D**: sniffing time in seconds, **water control 1**: aged: 0.70 ± 0.10; young: 0.81 ± 0.10; **water control 2**: aged: 0.31 ± 0.09; young: 0.48 ± 0.11; **La**: aged: 2.07 ± 0.43; young: 3.06 ± 0.35; **Lb**: aged: 0.64 ± 0.16; young: 0.74 ± 0.17; **Lc**: aged: 0.48 ± 0.10; young: 0.45 ± 0.10; **Oa**: aged: 1.23 ± 0.18; young: 1.22 ± 0.33; **Ob**: aged: 0.48 ± 0.13; young: 0.84 ± 0.13; **Oc**: aged: 0.49 ± 0.11; young: 0.55 ± 0.15), suggesting that self-recognition is overall preserved in senescent mice.

Social novelty is disrupted during pathological aging

Last, we explored whether the observed impairments in social odor exploration and discrimination may negatively impact social interaction in naturally aged and APP/PS1^{Het} mice. To this aim, we performed a three-chamber test (Nadler et al., 2004; Yang et al., 2011; **Figure 7A**) to assess general sociability and social novelty in senescent and APP/PS1^{Het} animals. Our data indicated a reduction in social novelty in middle age APP1/PS1^{Het} mice, which was not detected in 2 year-old animals (**Figure 7B-E**, **Sociability**, sniffing time in seconds, **E**: aged: 14.50 ± 1.90; young: 25.06 ± 2.96; APP/PS1^{WT}: 39.15 ± 3.63; APP/PS1^{Het}: 41.00 ± 4.07; **M1^{A}**: aged: 47.24 ± 4.60; young: 64.35 ± 5.23; APP/PS1^{WT}: 69.40 ± 6.05; APP/PS1^{Het}: 69.73 ± 7.10; **Social novelty**, sniffing time in seconds, **M1^{B}**: aged: 49.15 ± 4.20; young: 62.37 ± 5.01; APP/PS1^{WT}: 71.30 ± 5.75; APP/PS1^{Het}: 65.12 ± 6.70; **M2**: aged: 63.70 ± 5.30; young: 99.93 ± 9.83; APP/PS1^{WT}: 93.07 ± 11.70; APP/PS1^{Het}: 77.02 ± 8.43). Although senescent mice did not show significant impairments in either sociability or social novelty, they exhibited a mild increase in the latency to approach M1 during the sociability phase (**Supplementary Figure 10**), consistent with the overall decrease in the exploration time of social odors **(Figures 3, Supplementary Figures 3 and 4)**. These findings exposed exacerbated social deficits in an animal model of AD, suggesting a distinct impact of natural and pathological aging on social behavior.

Discussion

The quality of social life has been proposed as a predictive factor for developing dementia or mental illness (Cohen et al., 1985; Kawachi and Berkman, 2001; Stockdale et al., 2007; Moak and Agrawal, 2010; Wilson et al., 2007). However, the impairment of social functions with age is poorly understood

with some authors suggesting that social deficits might be the consequence of a more generalized brain impairment (Bottiroli et al., 2016; Johansson et al., 2018), but also an early manifestation of AD (Moran et al., 2012; Cavallini et al., 2013) which might be developed independently of cognitive deficits (Mohs et al., 2000; Spalletta et al., 2004).

Our results revealed that both natural and pathological aging affect several key aspects of social information processing in mice including the exploration of social odors, social odor discrimination and habituation. To gain insight into the mechanisms underlying these deficits, we explored the age-related adaptions of the VSE, a central gateway for pheromone-encoded information in mammals (Jacobson, 1813; Halpern and Martínez-Marcos, 2003; Munger et al., 2009). The accessory olfactory system has been indeed largely overlooked in contrast to other aspects of olfaction, whose functional decline has been suggested as a potential biomarker of neurodegenerative disorders like AD (recently reviewed in Murphy, 2019).

Our data showed VSE anatomical alterations during natural aging but not in APP/PS1^{Het} mice, a standardized animal model of AD. Whereas the VSE of APP/PS1^{Het} mice maintained fairly stable neurogenic capabilities, senescent wild type animals showed a significant reduction in proliferative and stem cells (PCNA^{+} and Sox2^{+} VSE cells) (**Figure 2**) which may explain the reduction of mature OMP^{+} neurons, sustentacular Sox2^{+} cells and VSE volume (**Figure 1** and **Supplementary Figure 1**). Our findings are consistent with two previous studies directly exploring the effects of natural aging in the VSE (Brann and Firestein, 2010; Mechin et al., 2021), which reported an overall thinning of the vomeronasal sensory epithelium (Mechin et al., 2021) and reduced VSE neurogenesis in 2-year-old animals (Brann and Firestein, 2010). Here, we expand this current knowledge by providing novel information on the properties of the VSE in a commonly used animal model of AD (APP/PS1^{Het}), revealing an unexpected preservation of the organ and its proliferative capabilities in middle age APP/PS1^{Het} mice. These results contrast with the reduction in SVZ neurogenesis reported in similar animal models (Scopa et al., 2020; Zeng et al., 2016; Verret et al., 2007; Zhang et al., 2007), suggesting that VSE neurogenesis might be less susceptible to lesions (Brann and Firestein, 2010) and pathological conditions than other proliferative areas. However, we cannot rule out the possibility that APP/PS1^{Het} animals may develop potential alterations in the VSE structure and cell composition at a later age (> 1 year-old). An aspect that we were prevented to investigate due to the life expectancy (~ 14-16 months-old) of this mouse model.

A relevant aspect of our work is that most previous studies addressing olfactory decline during natural and pathological aging employed synthetic and neutral odors, thus remaining uncertain the effect of healthy and diseased aging in the recognition of social cues. To gain insight into this question, we investigated the exploration time and the habituation-dishabituation response to social odors (urine) (**Figures 3, 5**). Our findings revealed that despite the distinctive effects of natural and pathological aging in VSE structure and neurogenic capability, both processes affected the exploration of socio-sexual information, social discrimination-habituation, and social behavior, suggesting fundamental differences in how these processes impact social information encoding.

Further experiments are needed to establish causality, but our results suggest that the observed VSE alterations in 2-year-old mice may elicit deficits in urine exploration time and the lack of habituation to intermediate urine dilutions (**Figure 3; Supplementary Figures 3 and 4**). VSE volume data from middle age APP/PS1^{WT} control animals may be suggestive that VSE structural changes might start to appear at a younger age (**Figure 1A**: VES volume mm^{3}: 4 month-old: 0.190 ± 0.008; 1-year-old APP/PS1^{WT}: 0.170 ± 0.007; $p = 0.03$; two-way ANOVA with Tuckey´s test), although their functional consequences might not become apparent until advanced stages of aging (2-year-old). This scenario suggests an aged-related parsimonious decay of the VNO that matches the reported effect of natural aging in other olfactory areas like the OB. Several studies have shown that despite the reduced regeneration rate of olfactory sensory neurons (OSNs), OB alterations involving a reduced number of

synaptic contacts (Richard et al., 2010), expression defects of odorant receptor genes (Lee et al., 2009; Khan et al., 2013) and changes in the OSNs dynamic range (Kass et al., 2018) are of late occurrence and just becoming obvious in 2-year-old mice. Although the olfactory system may undergo age-related changes from middle age (Mobley et al., 2014), functional deficits during natural aging might exhibit a late onset, suggesting compensatory mechanisms to preserve the processing of olfactory cues like social information relevant for the survival of aged animals (Tobiansky et al., 2012; Tikhonova et al., 2015). In contrast to the steadily decline of natural aging, pathological conditions may accelerate functional deficits even in the absence of obvious structural changes of peripheral organs like the VNO, suggesting impairments in the central processing of social information. In this regard, defects in the exploration of social odors were found exacerbated in APP/PS1^{Het} mice, which exhibited significant impairments already at middle age (**Figure 3, D-E**), a condition likely to aggravate frailty and reduce life expectancy in this animals (as observed in this mouse strain in our experimental conditions).

Furthermore, a detailed analysis of the first discrimination phase of the modified social habituation-dishabituation (presentation of S1a urine sample after 24 hours; **Figure 5, F-G**) revealed significant impairments in both 2-year old wild type animals and middle age APP/PS1^{Het} mice, suggesting that in parallel to peripheral sensory decline, the downstream pathways involved in social cue recognition may be affected during both natural and pathological aging. To control for a potential contribution of novelty in the social habituation-dishabituation test, we presented urine samples from littermate and novel animals finding similar deficits in discrimination (**Figure 6**). Interestingly, although senescent animals presented discrimination deficits they preserved the ability to differentiate between urine from a novel subject and their own, preventing to explore further the underlying mechanisms of subjective perception loss, a disrupting symptom of senescence and dementia which currently lacks appropriate animal models for preclinical studies (Jessen et al., 2020).

Age-related decline of olfactory detection is likely to occur due to alterations of both the main olfactory epithelium and the VNO (Apfelbach et al., 1991; Lee et al., 2009; Ueha et al., 2018), thus potentially affecting other odor modalities. Here, we sought to explore this question by performing odor-evoked sniffing tests employing social and neutral synthetic odors (**Figure 4**). Quantification of the exploration time across various IA dilutions exposed equivalent measurements in senescent and young mice, and even enhanced responses in the case of APP/PS1^{Het} mice. Furthermore, results from a food seeking test, exposed no significant differences in the latency time to find the hidden food pellets (**Figure 5E**) indicating that defects in social odor detection related to natural and pathological aging may be more severe than other odor modalities. A plausible explanation for the specific impairment in the exploration of social odors of aged and APP/PS1^{Het} animals may involve the reduction of reproductive activity in old animals, but not in foraging and feeding behaviors (Harb et al., 2014). The decline to detect specific odors may rise from alterations on the number of sensory neurons and synaptic connections specifically related to the discrimination of conspecifics (Wacker et al., 2010; Bielsky et al., 2005; Tobin et al., 2010) and heterospecific social cues (e.g. predator) (Kang et al., 2009; Wacker et al., 2010). In particular, impairments in social odor exploration and discrimination may rise from maladaptations specific to the VNO-AOB axis, consistent with the observed decrease in AOB volume in senescent animals (**Figure 1B**). Future studies should deepen into the anatomical and functional properties of the VNO-AOB circuit in order to obtain a complete picture on how healthy and pathological aging affect social information processing.

Finally, we sought to determine how the age-related defects in social odor sensitivity, discrimination and memory shaped social behavior. Results from a three chamber test (**Figure 7**) indicated that sociability was overall preserved in senescent and APP/PS1^{Het} animals. In contrast, social novelty was severely impaired in APP/PS1^{Het} mice consistently with previous studies (Cheng et al., 2014; Olesen et al., 2016; Locci et al., 2021; Shoji and Miyakawa, 2019). Deficits in social novelty in APP/PS1^{Het} mice could be linked to the deficits in social discrimination observed in the habituation-dishabituation test (**Figure 5D, E** and **Supplementary Figure 8;** Enwere et al., 2004; Patel and Larson, 2009; Moreno et

al., 2014) which could impair the recognition of M2 as a novel subject. Consistent with the overall decrease in the exploration time of social odors **(Figures 3, Supplementary Figures 3 and 4)**, aged animals exhibited a mild increase in the latency to approach the novel mouse (M1) during the first sociability phase (**Supplementary Figure 10**). These findings indicate that despite the reduction in social odor exploration and discrimination, overall sociability and novelty are majorly preserved in naturally aged mice. In contrast, the APP/PS1 neurodegenerative model shows a measurable impairment in social preference. This evidence opens the intriguing possibility that neuronal circuits underlying specific social functions (sociability vs social memory) may be particularly susceptible to pathological aging.

The present study offers new evidence on how natural and pathological aging distinctively impact the pheromone detection system and different aspects of social information processing, a necessary first step towards developing novel strategies to reduce the deterioration of olfactory deficits and social behavior in aged subjects.

Figure legends

Figure 1. Structural modifications of the mouse VSE during natural and pathological aging. A) Dispersion plot of the VSE volume indicates a significant reduction during natural but not pathological aging. **B)** Dispersion plot of AOB volume. Thick lines indicate the mean ± SEM. Data were obtained from 4 animals per condition. **C)** Representative images of OMP staining in the VSE during natural and pathological aging. Scale bar indicates 100 μm. **D)** Representative images of Sox2 staining in the VSE and the supporting cell layer. Scale bar indicates 100 μm. VL: vomeronasal lumen; SCL: supporting cell layer; NSE: non-sensory epithelium; M: marginal zone; I: intermediate zone; C: central zone. **E, F)** Dispersion plots represent the number of OMP^+ cells in the VSE (number of cells x $10^3/\mu m^3$) and the intensity of Sox2 fluorescence in the SCL (Sox2 CTF /μm^2). Thick lines indicate the mean ± SEM. Data were obtained from 10-16 slices from at least three animals per condition. Statistical comparisons were calculated by two-way ANOVA with Tukey´s test. * $P \leq 0.05$; ** $P \leq 0.01$; *** $P \leq 0.001$.

Figure 2. Natural and pathological aging differentially impact cell proliferation in the VSE. A) Representative confocal images of PCNA staining in the VSE proliferative niche during natural and pathological aging. To note there is no overlapping signal between the two markers indicating the identification of cells at different maturation stages (**Supplementary Figure 2**). Circles indicate the proliferative marginal region of the medial VNO. Scale bar represents 20 μm. **B, C)** Dispersion plots represent the number of $PCNA^+$ cells in the VSE (number of cells x $10^3/mm^3$) and the number of $Sox2^+$ cells in the VSE (number of cell x $10^4/\mu m^2$). Thick lines indicate the mean ± SEM. Data were obtained from ten slices from animal of each condition. Statistical analysis was calculated by two-way ANOVA with Tukey´s test for multiple comparisons. * $P \leq 0.05$; ** $P \leq 0.01$; *** $P \leq 0.001$.

Figure 3. Natural and pathological aging reduce exploration to social odors. A) Schematics of the olfactory test used in this study in which urine dilutions are presented as a social signal. **B)** Average of the exploration (sniffing) time of urine serial dilutions normalized to the exploration time of the vehicle (water) of adult and aged wild type mice. A typical habituation was observed in adult mice at intermediate dilutions (1:500, 1:250, 1:100; 1:50). **C)** Dispersion plot of the normalized sniffing time of each urine dilution (nd, non-diluted; 1:10; 1:50; 1:100; 1:250; 1:500; 1:1000) for adult and aged wild type mice. **D)** Average of the sniffing time of urine dilutions normalized to the exploration time of the vehicle (water) of middle age APP/PS1 controls (APP^{WT}) and middle age APP/PS1 heterozygous mice ($APP/PS1^{Het}$). **E)** Dispersion plots of normalized sniffing time of middle age APP^{WT} control and $APP/PS1^{Het}$ mice. Grey lines in the dispersion plots indicate mean ± SEM. Data were analyzed by a one-way ANOVA with Tukey´s test to test multiple comparisons with more than one variable. * $P \leq 0.05$; ** $P \leq 0.01$; *** $P \leq 0.001$; **** $P \leq 0.0001$.

Figure 4. Aging and neurodegeneration impact social odor recognition more severely than other odor modalities. A) Average of the sniffing time in response to a neutral synthetic odor (isoamyl acetate, IA) normalized to the vehicle (mineral oil) of young and aged wild type mice. **B)** Dispersion plots of normalized sniffing time in response to various dilutions of IA in young and aged wild type mice. **C)** Average of the sniffing time in response to a neutral synthetic odor (isoamyl acetate, IA) normalized to the vehicle (mineral oil) of middle age APP/PS1 controls (APP^{WT}) and middle age APP/PS1 heterozygous mice ($APP/PS1^{Het}$). **D)** Dispersion plots of normalized sniffing time in response to various dilutions of IA in $APP/PS1^{WT}$ and $APP/PS1^{Het}$ mice. Note that $APP/PS1^{Het}$ mice exhibit significantly longer exploration times for the $1{:}10^4$ and 1:100 IA dilutions. **E)** Food deprived animals performed a food seeking test (schematics on the right) which revealed equivalent latencies to find hidden food pellets as shown in the dispersion data plot (left panel). Thick lines in dispersion plots indicate mean ± SEM. Data were analyzed by a one-way ANOVA with Tukey´s test to test multiple comparisons with more than one variable. Number of mice: *Neutral odor sensitivity*: young: n = 19; aged: n = 27; middle age control: n = 10; middle age $APP/PS1^{Het}$: n = 13. *Food finding test*: young: n = 21; aged: n = 27; APP^{WT}: n = 20; APP^{Het}: n = 16. * $P \leq 0.05$; ** $P \leq 0.01$; *** $P \leq 0.001$; **** $P \leq 0.0001$.

Figure 5. Social odor discrimination and habituation are reduced in naturally aged and $APP/PS1^{Het}$ mice. A) Schematics of the social habituation-dishabituation test used in this study: after habituation to the experimental cage, the animal is exposed to the same urine sample three times (S1a-c) which induces a typical increase in exploration time (1st discrimination) to be followed by a reduction in the sniffing time (1st habituation). Dishabituation induced by a urine sample from a new subject (S2a) elicits a second round of discrimination - habituation. **B)** Average sniffing time of the social habituation-dishabituation test performed by young and aged wild type mice. **C)** Dispersion plot of the sniffing time corresponding to the social habituation-dishabituation test of young and aged animals. **D)** Average sniffing time of the social habituation-dishabituation test performed by middle age $APP/PS1^{WT}$ control and $APP/PS1^{Het}$ mice. **E)** Dispersion plot of the sniffing time corresponding to the social habituation-dishabituation test of middle age $APP/PS1^{WT}$ control and $APP/PS1^{Het}$ mice. **F**) The habituation-dishabituation test was modified to assess potential deficits in long-term discrimination due to natural or pathological aging by presenting the same S1a sample 24 hours after. **G**) Paired data corresponding to the sniffing time during the first and second (24 hours later) S1a presentation is plotted for each condition. Thick lines in dispersion plots and black dots in G indicate mean ± SEM. Data were analyzed by a one-way ANOVA with Tukey´s test to test multiple comparisons with more than one variable. * $P \leq 0.05$; ** $P \leq 0.01$; *** $P \leq 0.001$; **** $P \leq 0.0001$.

Figure 6. Age-related deficits in social discrimination and habituation are not influenced by previous experience. A) Average sniffing time of social habituation-dishabituation test in response to odors from novel (N) or littermate (L) subjects. **B)** Dispersion plot of the exploration time of aged and young animals in response to novel or littermate urine samples. **C)** Average sniffing time of social habituation-dishabituation test in response to littermate and the animal´s own urine (O). **D)** Dispersion plot of exploration time of aged and young animals in response to their own´s or littermate urine samples. Thick lines in dispersion plots indicate mean ± SEM. Number of mice: young: n = 21; aged: n = 23. Data were analyzed by a one-way ANOVA with Tukey´s test to test multiple comparisons with more than one variable. * $P \leq 0.05$; ** $P \leq 0.01$; *** $P \leq 0.001$; **** $P \leq 0.0001$.

Figure 7. Social novelty is disrupted during pathological aging. A) Schematics of the three chamber test used in this study to test sociability and social novelty. In the sociability phase the sniffing time of E and $M1^A$ are compared. Social novelty is estimated by quantifying the sniffing time of exploring $M1^B$ versus M2. **B)** Dispersion plots of the sniffing times of E-$M1^A$ (sociability) and $M1^B$-M2 (social novelty) for young wild type mice. **C)** Dispersion plots of the sniffing times of E-$M1^A$ (sociability) and $M1^B$-M2 (social novelty) for aged wild type mice. **D)** Dispersion plots of the sniffing times of E-$M1^A$ (sociability) and $M1^B$-M2 (social novelty) for middle age APP^{WT} mice. **E)** Dispersion plots of the

sniffing times of E-M1^{A} (sociability) and M1^{B}-M2 (social novelty) for middle age APP^{Het} mice. Black dots in the paired plots indicate mean ± SEM. Number of mice: young: n = 10; aged: n = 14; middle age control: n = 10; middle age APP/PS1^{Het}: n = 12. Data were analyzed by a one-way ANOVA with Tukey´s test to test multiple comparisons with more than one variable. * $P \leq 0.05$; ** $P \leq 0.01$; *** $P \leq 0.001$; **** $P \leq 0.0001$.

Supplementary Figure 1 (related to Figure 1). Structural modifications of the mouse VSE and AOB during natural and pathological aging. A) Schematics depicting the VNO divisions into marginal (M), intermediate (I) and central (C). **B-D)** Dispersion plots of the number of OMP^{+} cells in the marginal, intermediate and central zone of the VSE. Thick lines in the dispersion plots indicate mean ± SEM. Data were obtained from 10-16 slices from at least three animals per condition. Statistical comparisons were calculated by one-way ANOVA with Tukey´s test for multiple comparisons with a single variable. P value < 0.05 is considered significant. P values are indicated in the plot.

Supplementary Figure 2 (related to Figure 2). The proliferative niche of the VSE is reduced during natural, but not pathological aging. Representative confocal images of both OMP and PCNA staining in the VSE proliferative niche. To note there is no overlapping signal between the two markers indicating the identification of cells at different maturation stages. Circles indicate the proliferative marginal region of the VSE. Scale bar represents 20 μm. Data were obtained from ten slices from animal of each condition.

Supplementary Figure 3 (related to Figure 3). Statistical comparison of the exploration time between different ages for each dilution. Dispersion plots represent the sniffing time of 2, 6, 12 and 24 months-old animals for the various serial dilutions tested in Figure 3. Thick grey lines indicate mean ± SEM. Number of mice for each condition and the P values for each statistical comparison is indicated in the tables below. Data were analyzed by a one-way ANOVA with Tukey´s test to test multiple comparisons with more than one variable.

Supplementary Figure 4 (related to Figure 3). Statistical comparison of exploration time between different dilutions for each analyzed age. Dispersion plots represent the sniffing time and trend curves of 2, 6, 12 and 24 months-old animals for the various serial dilutions tested in Figure 3. Thick dots indicate mean ± SEM. P values for each statistical comparison is indicated in the tables on the right. Data were analyzed by a one-way ANOVA with Tukey´s test to test multiple comparisons with more than one variable.

Supplementary Figure 5 (related to Figure 3). Aged-related deficits in social odor exploration exhibit no significant sex differences. A) Average exploration (sniffing) time of urine serial dilutions of adult and aged female wild type mice. **B)** Average exploration (sniffing) time of urine serial dilutions of adult and aged male wild type mice. **C)** Dispersion plots of the sniffing time of urine dilutions that show significant impairments in female mice (nd, non-diluted; 1:10; 1:500; 1:1000). **D)** Dispersion plots of the sniffing time of the urine dilutions that show significant changes in male mice (nd, non-diluted; 1:250; 1:500; 1:1000). Plots indicate mean ± SEM. Number of mice: adult females: n = 13; adult males: n = 11; aged females: n = 14; aged males: n = 11. Data were analyzed by a one-way ANOVA with Tukey´s test to test multiple comparisons with more than one variable. * $P \leq 0.05$; ** $P \leq 0.01$; *** $P \leq 0.001$.

Supplementary Figure 6 (related to Figure 3). Statistical comparison of the exploration time between APP/PS1^{WT} and APP/PS1^{Het} for each dilution. Dispersion plots represent the sniffing time middle age of APP^{WT} and APP^{Het} mice for the various serial dilutions tested in Figure 3. Thick grey lines indicate mean ± SEM. Number of mice for each condition and the P values for each statistical comparison is indicated in the tables below. Data were analyzed by a one-way ANOVA with Tukey´s test to test multiple comparisons with more than one variable.

Supplementary Figure 7 (related to Figure 3). Statistical comparison of the exploration time between different dilutions for APP/PS1^{WT} and APP/PS1^{Het} mice. Dispersion plots represent the sniffing time and trend curves of middle age APP^{WT} and APP^{Het} mice for the various serial dilutions tested in Figure 3. Thick dots indicate mean ± SEM. P values for each statistical comparison is indicated in the tables on the right. Data were analyzed by a one-way ANOVA with Tukey´s test to test multiple comparisons with more than one variable.

Supplementary Figure 8 (related to Figure 5). Social discrimination is reduced during natural and pathological aging. A) Dispersion plots of the sniffing time of the first discrimination phase (H_2O-S1a) for young and aged wild type animals. **B**) Dispersion plots of the sniffing time of the second discrimination phase (S1c-S2a) for young and aged wild type animals. **C**) Dispersion plots of the slope values of the first and second discrimination phases of young and aged mice. **D)** Dispersion plots of the sniffing time of the first discrimination phase (H_2O-S1a) for of APP^{WT} and APP^{Het} mice. **E**) Dispersion plots of the sniffing time of the second discrimination phase (S1c-S2a) for of APP^{WT} and APP^{Het} mice. **F**) Dispersion plots of the slope values of the first and second discrimination phases of APP^{WT} and APP^{Het} mice. Black dots in **A, B, D**, and **E** and thick lines in **C** and **F** indicate mean ± SEM. Data were analyzed by one-way ANOVA with Tukey´s test. * $P \leq 0.05$; ** $P \leq 0.01$; *** $P \leq 0.001$.

Supplementary Figure 9 (related to Figure 5). Social habituation is diminished during natural and pathological aging. A) Dispersion plots of the sniffing time of the first habituation phase (S1a-S1b) for young and aged wild type animals. **B**) Dispersion plots of the sniffing time of the second habituation phase (S2a-S2b) for young and aged wild type animals. **C**) Dispersion plots of the slope values of the first and second habituation phases of young and aged mice. **D)** Dispersion plots of the sniffing time of the first habituation phase (S1a-S1b) for of APP^{WT} and APP^{Het} mice. **E**) Dispersion plots of the sniffing time of the second habituation phase (S2a-S2b) for of APP^{WT} and APP^{Het} mice. **F**) Dispersion plots of the slope values of the first and second habituation phases of APP^{WT} and APP^{Het} mice. Black dots in **A, B, D**, and **E** and thick lines in **C** and **F** indicate mean ± SEM. Data were analyzed by one-way ANOVA with Tukey´s test. * $P \leq 0.05$; ** $P \leq 0.01$; *** $P \leq 0.001$.

Supplementary Figure 10 (related to Figure 7). Latency to approach the first stranger (M1) in the three chamber sociability test is increased in naturally aged animals. A) The sociability phase of the three chamber test involves exposing the test animal to a stranger mouse (M1) for the first time, which elicits an increase in the exploration time in that side of the chamber. B) Dispersion plots of the latency to approach M1 during the first encounter of the sociability phase. Thick lines indicate mean ± SEM. Data were analyzed by one way-ANOVA with Tukey´s test. * $P \leq 0.05$.

Acknowledgements

This work was supported by grants of the Spanish Ministry of Science and Innovation SAF2017-82524-R and PID2020-113878RB-I00 (to S.J.), the "Severo Ochoa" Program for Centres of Excellence in R&D (SEV-2013-0317 and SEV-2017-0723), the Generalitat Valenciana Prometeo/2019/014 (to S.J.), and a FPI contract (BES-2017-081243) to A.P. We also are grateful to the teams of the Imaging and Animal Facilities at the Institute of Neuroscience, and all members of the Jurado and Chamero laboratories for their support during the realization of this work.

Author contributions

The project was led by S.J. Brain sample preparation, data acquisition, and analysis was done by A.P. Result interpretation, manuscript preparation, and editing was done by S.J., P.C. and A.P. with help of members from the Jurado Lab at the Instituto de Neurociencias (CSIC-UMH).

Declaration of interests

The authors declare no competing interests

References

Adolphs R. The neurobiology of social cognition. *Curr. Opin. Neurobiol*. 2001; **11**: 231–239.

Ahlenius H., Visan V., Kokaia M., Lindvall O., Koaia Z. Neuronal stem and progenitor cells retain their potential for proliferation and differentiation into functional neurons despite lower number in aged brain. *J Neurosci*. 2009; **29**: 4408-4419.

Apfelbach R., Russ D., Slotnick B.M. Ontogenic changes in odor sensitivity, olfactory receptor area and olfactroy receptor density in the rat. *Chem Senses.* 1991; **16**: 209–218.

Baum M.J, Kelliher K.R. Complementary roles of the main and accessory olfactory systems in mammalian mate recognition. *Annu Rev Physiol*. 2009; **71**:141-160.

Beynon R.J, Hurst J.L. Urinary proteins and the modulation of chemical scents in mice and rats. *Peptides*. 2004; **25**:1553-1563.

Bielsky I.F., Hu S-B., Ren X., Terwilliger E.F., Young L.J. The V1a vasopressin receptor is necessary and sufficient for normal social recognition: a gene replacement study. *Neuron*. 2005; **47**: 503–513.

Bottiroli S., Cavallini E., Ceccato I., Vecchi T., Lecce S. Theory of mind in aging: comparing cognitive and affective components in the faux pas test. *Arch. Gerontol*. Geriatr. 2016; **62**:152–162. 10.1016/j.archger.2015.09.009.

Brann J.H., Firestein S.J. Regeneration of new neurons is preserved in aged vomeronasal epithelia. *J Neuroscience*. 2010; **30**: 15686-15694.

Brennan P.A., Kendrick K.M. Mammalian social odours: attraction and individual recognition. *Philos Trans R Soc Lond B Biol Sci*. 2006; **361**: 2061-2078.

Brennan P.A., Zufall F. Pheromonal communication in vertebrates. *Nature*. 2006; **444**: 308-15.

Breton-Provencher V., Lemasson M., Peralta M.R. 3rd, Saghatelyan A. Interneurons produced in adulthood are required for the normal functioning of the olfactory bulb network and for the execution of selected olfactory behaviors. *J Neurosci*. 2009; **29**:15245-15257. doi: 10.1523/JNEUROSCI.3606-09.2009.

Cavallini E., Lecce S., Bottiroli S., Palladino P., Pagnin A. Beyond false belief: theory of mind in young, young-old and old-old adults. *Int. J. Aging Hum Dev*. 2013; **76**: 181–198. 10.2190/ag.76.3.a

Chamero P., Leinders-Zufall T., Zufall F. From genes to social communication: molecular sensing by the vomeronasal organ. *Trends Neurosci.* 2012; **35**: 597-606.

Chamero P., Weiss J., Alonso M.T., Rodríguez-Prados M., Hisatsune C., Mikoshiba K., Leinders-Zufall T., Zufall F. 2017. Type 3 inositol 1,4,5-trisphosphate receptor is dispensable for sensory activation of the mammalian vomeronasal organ. *Sci Rep*. 7:10260.

Cheetham S.A., Thom M.D., Jury F., Ollier W.E.R., Beynon R.J., Hurst J.L. The genetic basis of individual-recognition signals in the mouse. *Curr Biol*. 2007; **17**:1771-1777.

Cheng D., Spiro A.S., Jenner A.M., Garner B., Karl T. Long-term cannabidiol treatment prevents the development of social recognition memory deficits in Alzheimer's disease transgenic mice. *J. Alzheimers Dis*. 2014; **42**: 1383-1396, 10.3233/JAD-140921.

Cohen S., Wills T.A. Stress, social Support, and the buffering hypothesis. *Psychological bulletin*. 1985; **98**:310–357. WOS: A1985AQC4600006. pmid:3901065.

Deacon R.M.J., Koros E., Bornemann K.D., Rawlins J.N.P. Aged Tg2576 mice are impaired on social memory and open field habituation tests. *Behav. Brain Res.* 2009; **197**: 466-468. 10.1016/j.bbr.2008.09.042.

De La Rosa-Prieto C., Saiz-Sanchez D., Ubeda-Bañon I., Argandoña-Palacios L., Garcia-Muñozguren S., Martínez-Marcos A. Fate of marginal neuroblasts in the vomeronasal epithelium of adult mice. *J Comp Neurol*. 2009; **517**:723-736.

Devanand D.P. Olfactory identification deficits, cognitive decline and dementia in older adults. *Am J Geriatr Psychiatry*. 2016; **24**: 1151-1157.

Donovan N.J., Okereke O.I., Vannini P., Amariglio R.E., Rentz D.M., Marshall G.A., Johnson K.A., Sperling R.A. Association of higher cortical amyloid burden with loneliness in cognitively normal older adults. *JAMA Psychiatry*. 2016; **73**:1230-1237. doi: 10.1001/jamapsychiatry.2016.2657.

Dorph-Petersen K.A., Lewis D.A. Stereological approaches to identifying neuropathology in psychosis. *Biol Psychiatry*. 2011; **69**: 113-126. doi: 10.1016/j.biopsych.2010.04.030.

Doty R.L., Kamath V. The influences of age on olfaction: a review. *Front Psychol*. 2014; 5.20 doi: 10.3389/fpsyg.2014.00020.

Doty R.L., Shaman P., Applebaum S.L., Giberson R., Siksorski L., Rosenberg L. Smell identification ability: changes with age. *Science*. 1984; **226**: 1441-1443.

Enwere E., Shingo T., Gregg C., Fujikawa H., Ohta S., Weiss S. Aging results in reduced epidermal growth factor receptor signaling, diminished olfactory neurogenesis, and deficits in fine olfactory discrimination. *J Neurosci*. 2004; **24**: 8354-8365.

Ferrero D.M., Moeller L.M., Osakada T., Horio N., Li Q., Roy D.S., Cichy A., Spehr M., Touhara K., Liberles S.D. A juvenile mouse pheromone inhibits sexual behaviour through the vomeronasal system. *Nature*. 2013; **502**: 368-371.

Fortes-Marco L., Lanuza E., Martinez-Garcia F., Agustín-Pavón C. Avoidance and contextual learning induced by a kairomone, a pheromone and a common odorant in female CD1 mice. *Front Neurosci*. 2015; **9**: 336. doi: 10.3389/fnins.2015.00336.

Friard O., Gamba M. BORIS: A free, versatile open-source event-logging software for video/audio coding and live observations. *Methods Ecol Evol*. 2016; **7**:1325-1330. https://doi.org/10. 1111/2041-210X.12584.

Garratt M., Stockley P., Armstrong S.D., Beynon R.J., Hurst J.L. The scent of senescence: sexual signaling and female preference in house mice. *J Evol Biol*. 2011; **11**: 2398-2409.

Gheusi G., Cremer H., McLean H., Chazal G., Vincent J.D., Lledo P.M. Importance of newly generated neurons in the adult OB for odor discrimination. *Proc. Natl. Acad. Sci. U.S.A.* 2000; **97**: 1823-1828.

Giacobini P., Benedetto A., Tirindelli R., Fasolo A. Proliferation and migration of receptor neurons in the vomeronasal organ of the adult mouse. *Brain Res Dev Brain Res*. 2000; **123**: 33–40.

Graziadei P.P., Monti-Graziadei A.G. Regeneration in the olfactory system of vertebrates. *Am J Otolaryngol.* 1983; **4**:228-33.

Guo Z., Packard A., Krolewski R.C., Harris M.T., Manglapus G.L., Schwob J.E. Expression of pax6 and sox2 in adult olfactory epithelium. J Comp Neurol. 2010; 18:4395-4418.

Halpern M., Martínez-Marcos A. Structure and function of the vomeronasal system: an update. *Prog Neurobiol*. 2003; **70**: 245-318.

Harb M.R., Sousa N., Zihl J., Almeida O.F.X. Reward components of feeding behavior are preserved during mouse aging. *Frontiers in Aging Neuroscience*. 2014; **6**:242.

Heinrichs M., Baumgartner T., Kirschbaum C., Ehlert U. Social support and oxytocin interact to suppress cortisol and subjective responses to psychosocial stress. *Biol Psychiatry*. 2003; 54:1389-1398. doi: 10.1016/s0006-3223(03)00465-7.

Hlinák Z., Krejcí I. Social recognition in male rats: age differences and modulation by MIF-I and alaptide. *Physiol Res*. 1991; **40**: 59-67.

Jacobson L. Anatomisk beskrivelse over et nyt organ I huusdyrenes naese. *Veter Salesk Skr*. 1813; **2**: 209-246.

Jagetia S., Milton A.J., Stetzik L.A., Liu S., Pai K., Arakawa K., Mandairon N., Wesson D.W. Inter- and intra-mouse variability in odor preferences revealed in an olfactory multiple-choice test. *Behav Neurosci*. 2018; **132**: 88-98.

Jankowsky J.L., Fadale D.J., Anderson J., Xu G.M., Gonzales V., Jenkins N.A., Copeland N.G., Lee M.K., Younkin L.H., Wagner S.L., Younkin S.G., Borchelt D.R. Mutant presenilins specifically elevate the levels of the 42 residue beta-amyloid peptide in vivo: evidence for augmentation of a 42-specific gamma secretase. *Hum Mol Genet*. 2004; **13**: 159-170.

Jankowsky J.L., Slunt H.H., Ratovitski T., Jenkins N.A., Copeland N.G., Borchelt D.R. Co-expression of multiple transgenes in mouse CNS: a comparison of strategies. *Biomol Eng*. 2001; **17**: 157-165.

Jessen F., Amariglio R.E., Buckley R.F., van der Flier W.M., Han Y., Molinuevo J.L., Rabin, L., Rentz D.M., Rodríguez-Gómez O., Saykin A.J., Sikkes S.A.M., Smart C.M., Wolfsgruber S., Wagner M. The characterisation of subjective cognitive decline. *Lancet Neurol*. 2020; **19**: 271-278. doi: 10.1016/S1474-4422(19)30368-0.

Johansson N.E., Murray K., Happé F., Charlton R.A. Cognitive and affective associations with an ecologically valid test of theory of mind across the lifespan. *Neuropsychology*. 2018; **32**: 754-763. 10.1037/neu0000464.

Kang N., Baum M.J., Cherry J.A. A direct main olfactory bulb projection to the 'vomeronasal' amygdala in female mice selectively responds to volatile pheromones from males. *Eur. J. Neurosci*. 2009; **29**: 624-634.

Kass M.D., Czarnecki L.A., McGann J.P. Stable olfactory sensory neuron in vivo physiology during normal aging. *Neurobiol Aging*. 2018; **69**: 33-37.

Katreddi R.R., Forni P.E. Mechanisms underlying pre- and postnatal development of the vomeronasal organ. *Cell Mol Life Sci*. 2021; **78**:5069-5082.

Kawachi I., Berkman L.F. Social ties and mental health. *Journal of Urban Health-Bulletin of the New York Academy of Medicine*. 2001; **78**: 458-467. WOS:000170919900005. pmid:11564849.

Khan M., Vaes E., Mombaerts P. Temporal patterns of odorant receptor gene expression in adult and aged mice. *Mol Cell Neurosci*. 2013; **57**: 120-129.

Kobayakawa K., Kobayakawa R., Matsumoto H., Oka Y., Imai T., Ikawa M., okabe M., Ikeda T., Itohara S., Kikusui T., Mori K., Sakano H. Innate versus learned odour processing in the mouse olfactory bulb. *Nature*. 2007; **450**: 503–508.

Kurien B.T., Everds N.E., Scofield R.H. Experimental animal urine collection: a review. *Laboratory Animals*. 2004; **38**: 333-361.

Lazarov O., Marr R.A. Neurogenesis and Alzheimer's disease: at the crossroads. *Exp Neurol*. 2010; **223**: 267-281.

La Joie R., Perrotin A., Egret S., Pasquier F., Tomadesso C., Mézenge F., Desgranges B., de La Sayette V., Chételat G. Qualitative and quantitative assessment of self-reported cognitive difficulties in nondemented elders: Association with medical help seeking, cognitive deficits, and β-amyloid imaging. *Alzheimers Dement (Amst).* 2016; **5**:23-34.

Lee A.C., Tian H., Grosmaitre X., Ma M. Expression patterns of odorant receptors and response properties of olfactory sensory neurons in aged mice. *Chem Senses*. 2009; **34**: 695-703.

Li Y., Dulac C. Neural coding of sex-specific social information in the mouse brain. *Curr Opin Neurobiol*. 2018; **53**: 120-130.

Locci A., Orellana H., Rodríguez G., Gottliebson M., McClarty B., Domínguez S., Keszycki R., Dong H. Comparison of memory, affective behavior, and neuropathology in APPNLGF knock-in mice to 5xFAD and APP/PS1 mice. *Behavioural Brain Research*. 2021; **404**: 113192.

Mandairon N., Poncelet J., Bensafi M., Didier A. Humans and mice express similar olfactory preferences. *PLoS ONE*. 2009; **4**:e4209.

Martínez B., Karunanayaka P., Wang J., Tobia M.J., Vasavada M., Eslinger P.J., Yang Q.X. Different patterns of age-related central olfactory decline in men and women as quantified by olfactory fMRI. *Oncotarget*. 2017; **8**: 79212-79222.

Mechin V., Pageat P., Teruel E., Asproni P. Histological and Immunohistochemical Characterization of Vomeronasal Organ Aging in Mice. *Animals*. 2021; **11**: 1211.

Moak Z.B., Agrawal A. The association between perceived interpersonal social support and physical and mental health: results from the national epidemiological survey on alcohol and related conditions. *J Public Health-Uk*. 2010; **32**: 191-201.

Mobley A.S., Rodriguez-Gil D.J., Imamura F., Greer C.A. Aging in the olfactory system. *Trends Neurosci*. 2014; **37**: 77-84.

Mohs R.C., Schmeidler J., Aryan M. Longitudinal studies of cognitive, functional and behavioural changes in patients with Alzheimer´s disease. *Sta Med*. 2000; **19**:1401-1409.

Moran J.M., Jolly E., Mitchell J.P. Social-cognitive deficits in normal aging. *J. Neurosci*. 2012; **32**: 5553–5561. 10.1523/JNEUROSCI.5511-11.2012

Moreno M., Richard M., Landrein B., Sacquet J., Didier A., Mandairon N. Alteration of olfactory perceptual learning and its cellular basis in aged mice. *Neurobiol Aging*. 2014; http://dx.doi.org/10.1016/j.neurobiolaging.2013.08.034.

Munger S.D, Leinders-Zufall T., Zufall F. Subsystem organization of the mammalian sense of smell. *Annu Rev Physiol*. 2009; **71**: 115-140.

Murphy C. Olfactory and other sensory impairments in Alzheimer disease. *Nat Rev Neurol*. 2019; **15**: 11-24.doi:10.1038/s41582-018-0097-5.

Murphy C., Schubert C.R., Cruickshanks K.J., Klein B.E.K., Klein R., Nondahl D.M. Prevalence of olfactory impairment in older adults. *JAMA*. 2002; **288**: 2307-2312.

Nadler J.J., Moy S.S., Dold G., Trang D., Simmons N., Perez A., Young N.B., Barbaro R.P., Piven J., Magnuson T.R., Crawley J.N. Automated apparatus for quantitation of social approach behaviors in mice. *Genes Brain Behav*. 2004; **3**: 303-314. doi: 10.1111/j.1601-183X.2004.00071.x.

Noack J., Richter K., Laube G., Haghgoo H.A., Veh R.W., Engelmann M. Different importance of the volatile and non-volatile fractions of an olfactory signature for individual social recognition in rats versus mice and short-term versus long-term memory. *Neurobiol. Learn. Mem*. 2010; **94**: 568-575.

Olesen L.Ø, Bouzinova E.V., Severino M., Sivasaravanaparan M., Hasselstrøm J.B., Finsen B., Wiborg O. Behavioural phenotyping of APPswe/PS1δE9 mice: Age related changes and effect of long-term paroxetine treatment. *PLoS One*, 2016; **11**: e0165144, 10.1371/journal.pone.0165144 PMID: 27814403.

Oboti L., Ibarra-Soria X., Perez-Gomez A., Schimd A., Pyrski M., Paschek N., Kircher S., Logan D.W., Leinders-Zufall T., Zufall F., Chamero P. Pregnancy and estrogen enhance neural progenitor-cell proliferation in the vomeronasal sensory epithelium. *BMC Biol* 2015; **13**: 104 doi: 10.1186/s12915-015-0211-8.

Panaliappan T.K., Wittmann W., Jidigam V. K,. Mercurio S., Bertolini J.A., Sghari S., Bose R., Patthey C., Nicolis S.K., Gunhaga L. Sox2 is required for olfactory pit formation and olfactory neurogenesis through BMP restriction and Hes5 upregulation. *Development*. 2018; **145**: dev153791.

Parrish-Aungst S., Shipley M.T., Erdelyi F., Szabo G., Puche A.C. Quantitative analysis of neuronal diversity in the mouse olfactory bulb. *J Comp Neurol*. 2007; **501**:825-836.

Patel R.C., Larson J. Impaired olfactory discrimination learning and decreased olfactory sensitivity in aged C57Bl/6 mice. *Neurobiol Aging*. 2009; **30**: 829-837.

Petrulis A., Johnston. Causes of scent making in female golden hamsters (Mesocricetus auratus): specific signals or classes of information? *J Comp Psychol*. 1997; **111**:25-36.

Rawson N.E., Gomez G., Cowart B.J., Kriete A., Pribitkin E., Restrepo D. Age-associated loss of selectivity in human olfactory sensory neurons. *Neurobiol Aging*. 2012; **33**: 1913-1919.

Reiserer R.S., Harrison F.E., Syverud D.C., McDonald M.P. Impaired spatial learning in the APPSwe + PSEN1DeltaE9 bigenic mouse model of Alzheimer´s disease. *Genes Brain Behav*. 2007; **6**: 54-65.

Richard M.B., Taylor S.R., Greer C.A. Age-induced disruption of selective olfactory bulb synaptic circuits. *Proc Natl Acad Sci U S A*. 2010; **107**: 15613-15618.

Roberts R.O., Christianson T.J., Kremers W.K., Mielke M.M., Machulda M.M., Vassilaki M., Alhurani R.E., Geda Y.E., Knopman D.S., Petersen R.C. Association between olfactory dysfunction and amnestic mild cognitive impairment and Alzheimer disease dementia. *JAMA Neurol*. 2016; **73**: 93-101. doi: 10.1001/jamaneurol.2015.2952

Root C.M., Denny C.A., Hen R., Axel R. The participation of cortical amygdala in innate, odour-driven behaviour. *Nature*. 2014; **515**: 269-273. doi: 10.1038/nature13897.

Sanderson D.J., Bannerman D.M. Competitive short-term and long-term memory processes in spatial habituation. *J Exp Psychol Anim Behav Process*. 2011; **37**:189-199. doi: 10.1037/a0021461.

Saraiva L.R., Kondoh K., Ye X., Yoon K.H., Hernandez M., Buck L.B. Combinatorial effects of odorants on mouse behavior. *Proc Natl Acad Sci U S A.* 2016; **113**: E3300-E3306.

Scopa C., Marrocco F., Latina V., Ruggeri F., Corvaglia V., La Regina F., Ammassari-Teule M., Middei S., Amadoro G., Meli G., Scardigli R., Cattaneo A.. Impaired adult neurogenesis is an early event in

Alzheimer's disease neurodegeneration, mediated by intracellular Aβ oligomers. *Cell Death Difer*. 2020; **27**: 934-948.

Shipley M.T., Ennis M., Puche A.C. The olfactory system. In: Conn, P.M. (Ed.), *Neuroscience in Medicine. Humana Press*, Totowa. 2008: 611-622.

Spalletta G., Baldinetti, Buccione I., Fadda L., Perri R., Scalmana S., Serra L., Caltagirone. Cognition and behaviour are independente and hetreogenous dimensions in Alzheimer´s disease. *J Neurol*. 2004; **251**: 688-695.

Stockdale S.E., Wells K.B., Tang L., Belin T.R., Zhang L., Sherbourne C.D. The importance of social context: Neighborhood stressors, stress-buffering mechanisms, and alcohol, drug, and mental health disorders. *Social Science & Medicine*. 2007; **65**:1867-1881.

Taroc E.Z.M., Katreddi R.R., Forni P.E. Identifying Isl1 genetic lineage in the developing olfactory system and in GnRH-1 neurons. *Front Physiol*. 2020 **11**:601923.

Tikhonova M.A., Romaschenko A.V., Akulov A.E., Ho Y.J., Kolosova N.G., Moshkin M.P., Amstislavskaya T.G. Comparative study of perception and processing of socially or sexually significant odor information in male rats with normal or accelerated senescence using fMRI. *Behav Brain Res*. 2015; **294**:89-94. doi: 10.1016/j.bbr.2015.08.001.

Tobiansky D.J., Hattori T., Scott J.M., Nutsch V.L., Roma P.G., Dominguez J.M. Mating-relevant olfactory stimuli activate the rat brain in an age-dependent manner. *Neuroreport*. 2012; **23**:1077-1083. doi: 10.1097/WNR.0b013e32835b6ec1.

Tobin V.A., Hashimoto H., Wacker D.W., Takayanagi Y., Langnaese K., Caquineau C., Noack J., landgrave R., Onaka T., Leng G., Meddle S.L., Engelmann M., Ludwig M. An intrinsic vasopressin system in the olfactory bulb is involved in social recognition. *Nature*. 2010; **464**: 413-417.

Tucker E.S., Lehtinen M.K., Maynard T., Zirlinger M., Dulac C., Rawson N., Pevny L., La-Mantia A.S. Proliferative and transcriptional identity of distinct classes of neural precursors in the mammalian olfactory epithelium. *Development*. 2010; **137**: 2471-2481. doi: 10.1242/dev.049718.

Ueha R., Shichino S., Ueha S., Kondo K., Kikuta S., Nishijima H., Matsushima K., Yamasoba T. Reduction of proliferating olfactory cells and low expression of extracellular matrix genes are hallmarks of the aged olfactory mucosa. *Front Aging Neurosci*. 2018; **10**:86. doi: 10.3389/fnagi.2018.00086.

Valech N., Tort-Merino A., Coll-Padrós N., Olives J., León M., Rami L, Molinuevo J.L. Executive and language subjective cognitive decline complaints discriminate preclinical Alzheimer's disease from normal aging. *J Alzheimers Dis*. 2018; **61**:689-703.

Verret L., Jankowsky J.L., Xu G.M., Borchelt D.R., Rampon C. Alzheimer's-type amyloidosis in transgenic mice impairs survival of newborn neurons derived from adult hippocampal neurogenesis. *J Neurosci*. 2007; **27**: 6771-6780.

Wacker D.W., Tobin V.A., Noack J., Bishop V.R., Duszkiewicz A.J., Engelmann M., Meddle S.L., Ludwig M. Expression of early growth response protein 1 in vasopressin neurones of the rat anterior olfactory nucleus following social odour exposure. *J. Physiol*. 2010; **588**: 4705-4717.

Weiler E. Postnatal development of the rat vomeronasal organ. *Chem Senses*. 2005; **30**: i127-8. 2. doi: 10.1093/chemse/bjh147.

Weiler E., McCulloch M.A., Farbman A.I. Proliferation in the vomeronasal organ of the rat during postnatal development. *Eur J Neurosci*. 1999; **11**: 700-711.

West M.J., Gundersen H.J. Unbiased stereological estimation of the number of neurons in the human hippocampus. *J Comp Neurol*. 1990; **296**:1-22.

Whitman M.C., Greer C.A. Adult neurogenesis and the olfactory system. *Prog Neurobiol*. 2009; **89**:162-75.

Wilson R.S., Krueger K.R., Arnold, S.E., Schneider J.A., Kelly J.F., Barnes L.L., Tang Y., Bennett D.A. Loneliness and risk of Alzheimer disease. *Arch Gen Psychiatry*. 2007; **64**: 234-240. doi: 10.1001/archpsyc.64.2.234.

Wong F.K., Bercsenyi K., Sreenivasan V., Portalés A., Fernández-Otero M., Marín O. Pyramidal cell regulation of interneuron survival sculpts cortical networks. *Nature*. 2018; **557**: 668-673. doi: 10.1038/s41586-018-0139-6.

Xu F., Schaefer M., Kida I., Schafer J., Liu N., Rothman D.L., Hyder F., Restrepo D., Shepherd G.M. Simultaneous activation of mouse main and accessory olfactory bulbs by odors or pheromones. *J Comp Neurol*. 2005; **489**: 491-500. doi: 10.1002/cne.20652.

Yang M., Crawley J.N. Simple behavioral assessment of mouse olfaction. *Curr Protoc Neurosci*. 2009. **8**: doi: 10.1002/0471142301.ns0824s48.

Yang M., Silverman J.L., Crawley J.N. Automated three-chambered social approach task for mice. *Curr Protoc Neurosci*. 2011. **8**: 8.26. doi: 10.1002/0471142301.ns0826s56.

Yoon H., Enquist L.W., Dulac C. Olfactory inputs to hypothalamic neurons controlling reproduction and fertility. *Cell*. 2005; **123**: 669-82.

Zeng Q., Zheng M., Zhang T., He G. Hippocampal neurogenesis in the APP/PS1/nestin-GFP triple transgenic mouse model of Alzheimer´s disease. *Neuroscience*. 2016; **314**: 64-74. doi: 10.1016/j.neuroscience.2015.11.054.

Zhang C., McNeil E., Dressler L., Siman R. Long-lasting impairment in hippocampal neurogenesis associated with amyloid deposition in a knock-in mouse model of familial Alzheimer's disease. *Exp Neurol*. 2007; **204**: 77-87.

Zufall F., Leinders-Zufall T. Mammalian pheromone sensing. *Curr Opin Neurobiol*. 2007; **17**:483-9.

FIGURE 1

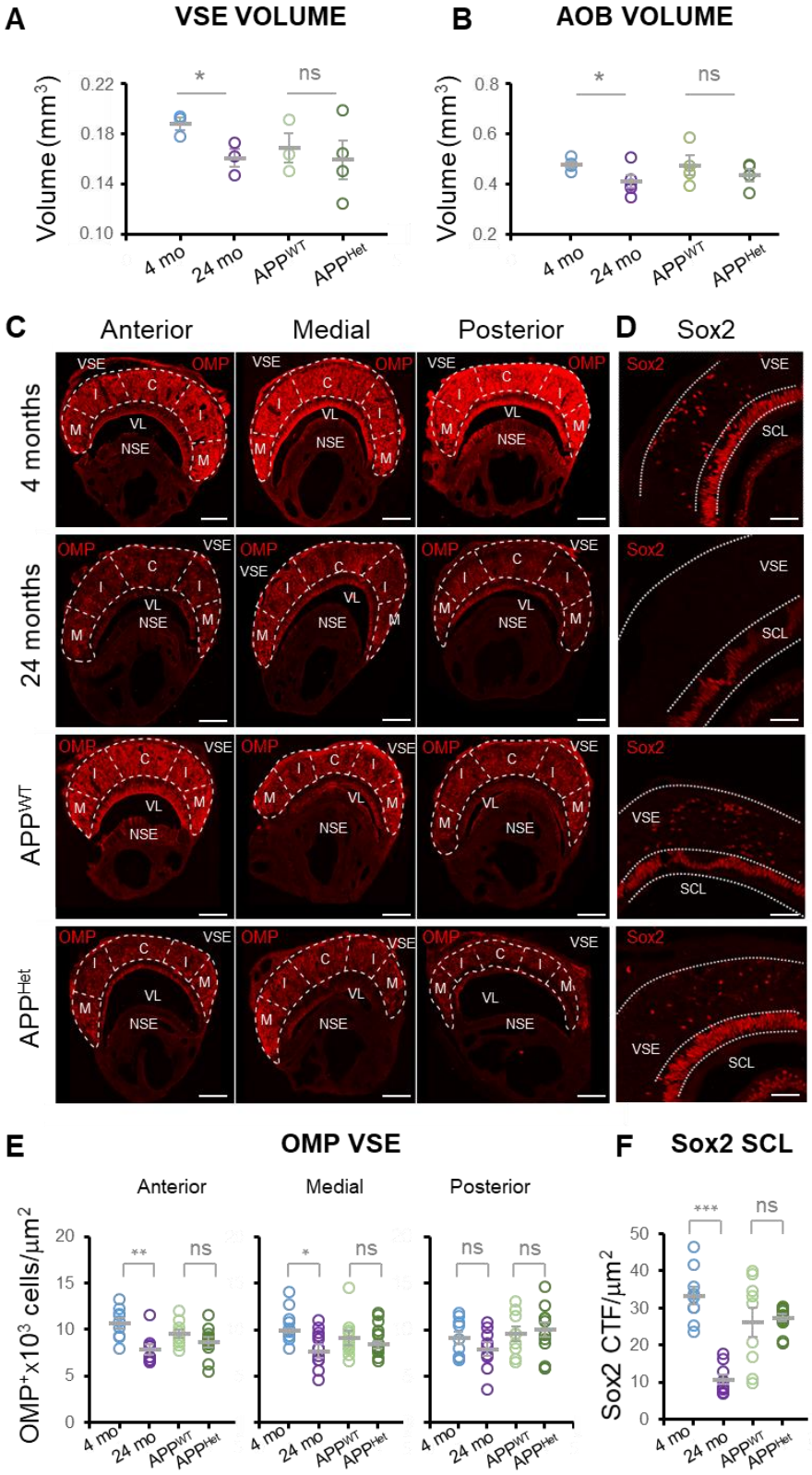

Figure 1. Structural modifications of the mouse VSE during natural and pathological aging. **A)** Dispersion plot of the VSE volume indicates a significant reduction during natural but not pathological aging. **B)** Dispersion plot of AOB volume. Thick lines indicate the mean ± SEM. **C)** Representative images of OMP staining in the VSE during natural and pathological aging. Scale bar indicates 100 µm. **D)** Representative images of Sox2 staining in the VSE and the supporting cell layer. Scale bar indicates 100 µm. VL: vomeronasal lumen; SCL: supporting cell layer; NSE: non-sensory epithelium; M: marginal zone; I: intermediate zone; C: central zone. **E, F)** Dispersion plots represent the number of OMP^+ cells in the VSE (number of cells x $10^3/\mu m^3$) and the intensity of Sox2 fluorescence in the SCL (Sox2 CTF $/\mu m^2$). Thick lines indicate the mean ± SEM. Data were obtained from 10-16 slices from at least three animals per condition. Statistical comparisons were calculated by two-way ANOVA with Tukey´s test. * $P \leq 0.05$; ** $P \leq 0.01$; *** $P \leq 0.001$.

FIGURE 2

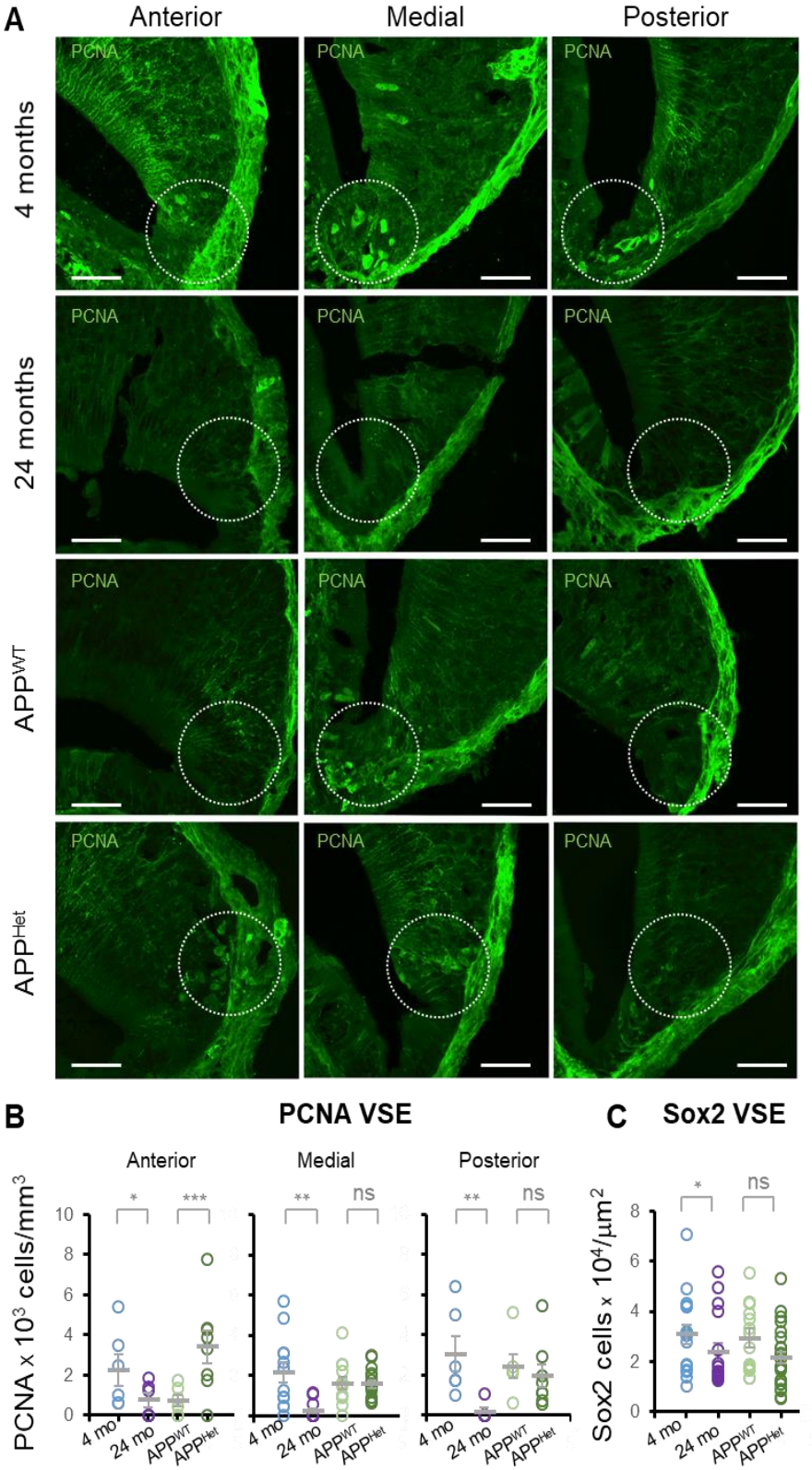

Figure 2. Natural and pathological aging differentially impact cell proliferation in the VSE. A) Representative confocal images of PCNA staining in the VSE proliferative niche during natural and pathological aging. To note there is no overlapping signal between the two markers indicating the identification of cells at different maturation stages (**Supplementary Figure 2**). Circles indicate the proliferative marginal region of the medial VNO. Scale bar represents 20 µm. **B, C)** Dispersion plots represent the number of PCNA$^+$ cells in the VSE (number of cells x 10^3/mm^3) and the number of Sox2$^+$ cells in the VSE (number of cell x 10^4/µm^2). Thick lines indicate the mean ± SEM. Data were obtained from ten slices from animal of each condition. Statistical analysis was calculated by two-way ANOVA with Tukey´s test for multiple comparisons. * $P \leq 0.05$; ** $P \leq 0.01$; *** $P \leq 0.001$.

FIGURE 3

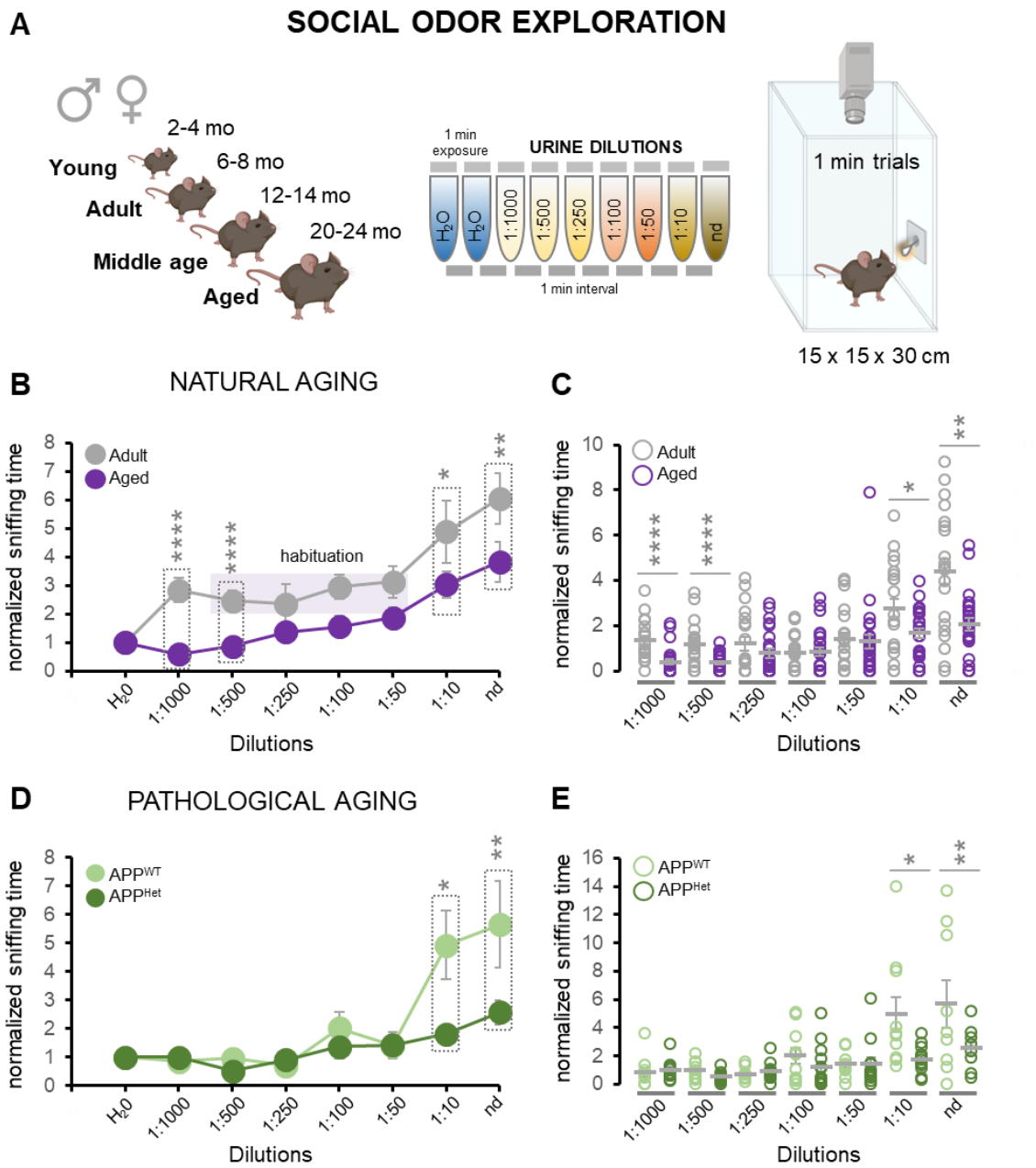

Figure 3. Natural and pathological aging reduce exploration to social odors. A) Schematics of the olfactory test used in this study in which urine dilutions are presented as a social signal. **B)** Average of the exploration (sniffing) time of urine serial dilutions normalized to the exploration time of the vehicle (water) of adult and aged wild type mice. A typical habituation was observed in adult mice at intermediate dilutions (1:500, 1:250, 1:100; 1:50). **C)** Dispersion plot of the normalized sniffing time of each urine dilution (nd, non-diluted; 1:10; 1:50; 1:100; 1:250; 1:500; 1:1000) for adult and aged wild type mice. **D)** Average of the sniffing time of urine dilutions normalized to the exploration time of the vehicle (water) of middle age APP/PS1 controls (APP^{WT}) and middle age APP/PS1 heterozygous mice ($APP/PS1^{Het}$). **E)** Dispersion plots of normalized sniffing time of middle age APP^{WT} control and $APP/PS1^{Het}$ mice. Grey lines in the dispersion plots indicate mean ± SEM. Data were analyzed by a one-way ANOVA with Tukey´s test to test multiple comparisons with more than one variable. * $P \leq 0.05$; ** $P \leq 0.01$; *** $P \leq 0.001$; **** $P \leq 0.0001$.

FIGURE 4

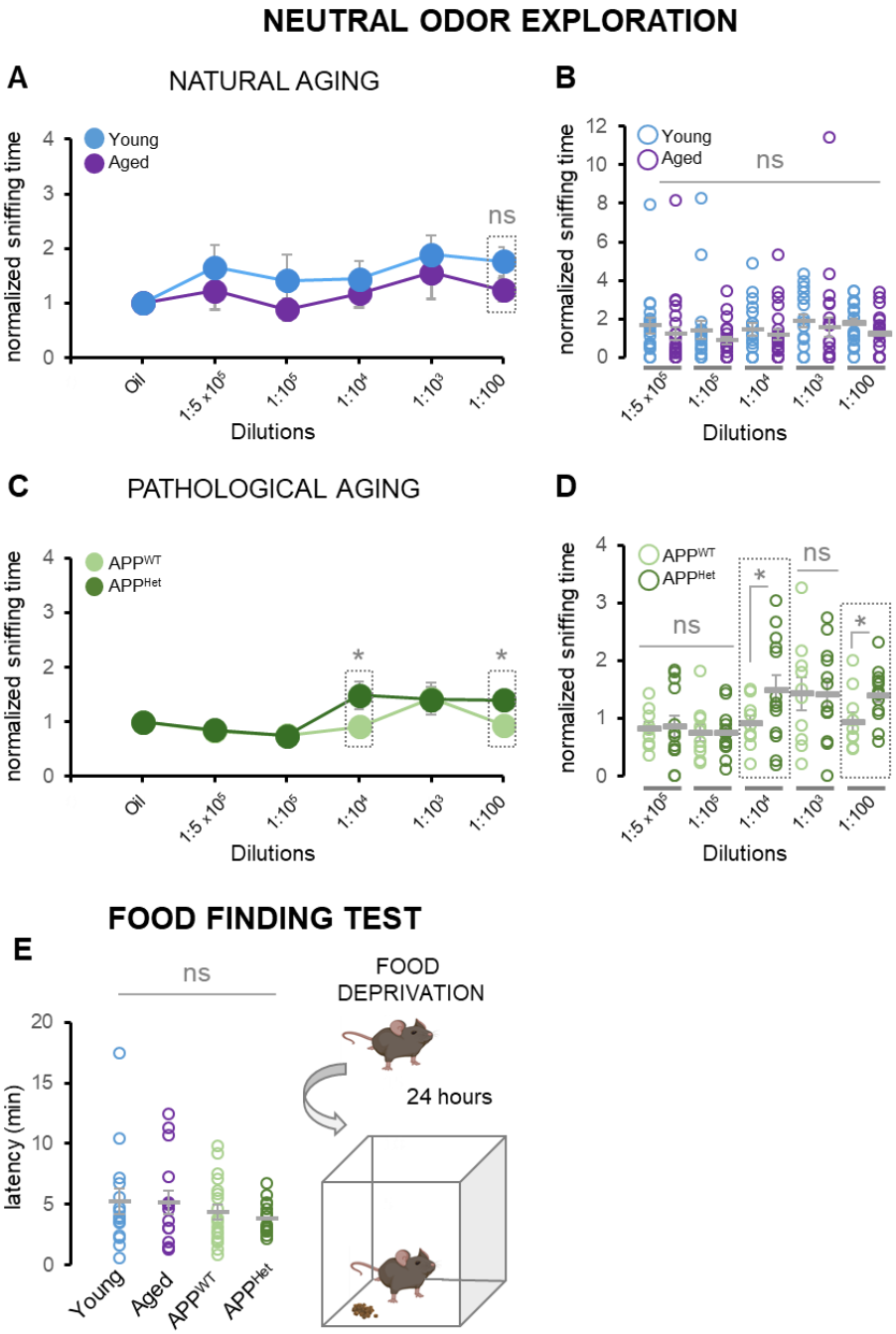

Figure 4. Aging and neurodegeneration impact social odor recognition more severely than other odor modalities. A) Average of the sniffing time in response to a neutral synthetic odor (isoamyl acetate, IA) normalized to the vehicle (mineral oil) of young and aged wild type mice. **B)** Dispersion plots of normalized sniffing time in response to various dilutions of IA in young and aged wild type mice. **C)** Average of the sniffing time in response to a neutral synthetic odor (isoamyl acetate, IA) normalized to the vehicle (mineral oil) of middle age APP/PS1 controls (APP^{WT}) and middle age APP/PS1 heterozygous mice ($APP/PS1^{Het}$). **D)** Dispersion plots of normalized sniffing time in response to various dilutions of IA in $APP/PS1^{WT}$ and $APP/PS1^{Het}$ mice. Note that APP/PS1Het mice exhibit significantly longer exploration times for the 1:104 and 1:100 IA dilutions. **E)** Food deprived animals performed a food seeking test (schematics on the right) which revealed equivalent latencies to find hidden food pellets as shown in the dispersion data plot (left panel). Thick lines in dispersion plots indicate mean ± SEM. Data were analyzed by a one-way ANOVA with Tukey´s test to test multiple comparisons with more than one variable. Number of mice: Neutral odor sensitivity: young: n = 19; aged: n = 27; middle age APP^{WT}: n = 10; middle age $APP/PS1^{Het}$: n = 13. Food finding test: young: n = 21; aged: n = 27; APP^{WT}: n = 20; APP^{Het}: n = 16. * $P \leq 0.05$; ** $P \leq 0.01$; *** $P \leq 0.001$; **** $P \leq 0.0001$.

FIGURE 5

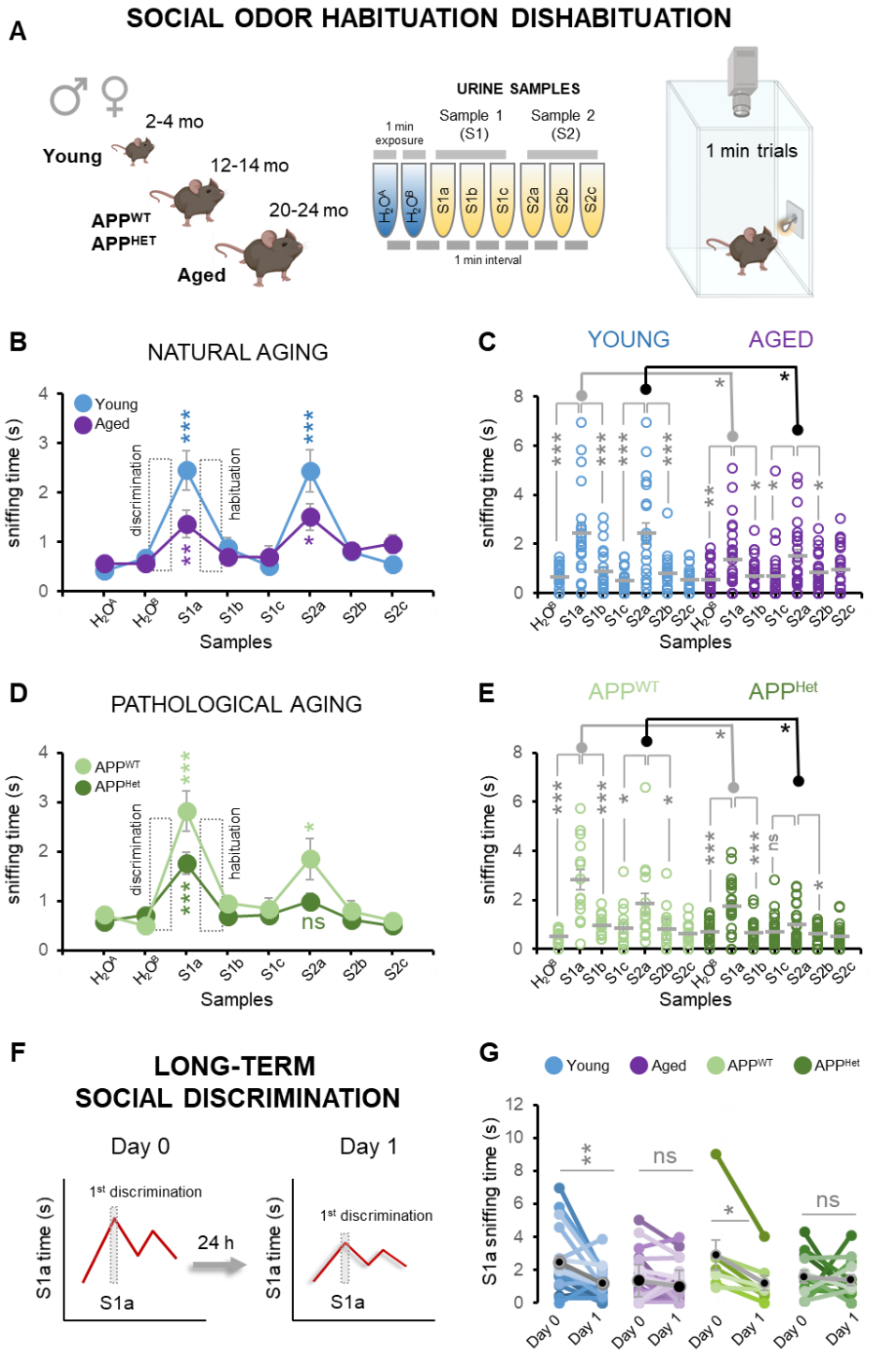

Figure 5. Social odor discrimination and habituation are reduced in naturally aged and APP/PS1^{Het} mice. A) Schematics of the social habituation-dishabituation test used in this study: after habituation to the experimental cage, the animal is exposed to the same urine sample three times (S1a-c) which induces a typical increase in exploration time (1st discrimination) to be followed by a reduction in the sniffing time (1st habituation). Dishabituation induced by a urine sample from a new subject (S2a) elicits a second round of discrimination - habituation. **B)** Average sniffing time of the social habituation-dishabituation test performed by young and aged wild type mice. **C)** Dispersion plot of the sniffing time corresponding to the social habituation-dishabituation test of young and aged animals. **D)** Average sniffing time of the social habituation-dishabituation test performed by middle age APP/PS1^{WT} control and APP/PS1^{Het} mice. **E)** Dispersion plot of the sniffing time corresponding to the social habituation-dishabituation test of middle age APP/PS1^{WT} control and APP/PS1^{Het} mice. **F)** The habituation-dishabituation test was modified to assess potential deficits in long-term discrimination due to natural or pathological aging by presenting the same S1a sample 24 hours after. **G)** Paired data corresponding to the sniffing time during the first and second (24 hours later) S1a presentation is plotted for each condition. Thick lines in dispersion plots and black dots in G indicate mean ± SEM. Data were analyzed by a one-way ANOVA with Tukey´s test to test multiple comparisons with more than one variable. * $P \leq 0.05$; ** $P \leq 0.01$; *** $P \leq 0.001$; **** $P \leq 0.0001$.

FIGURE 6

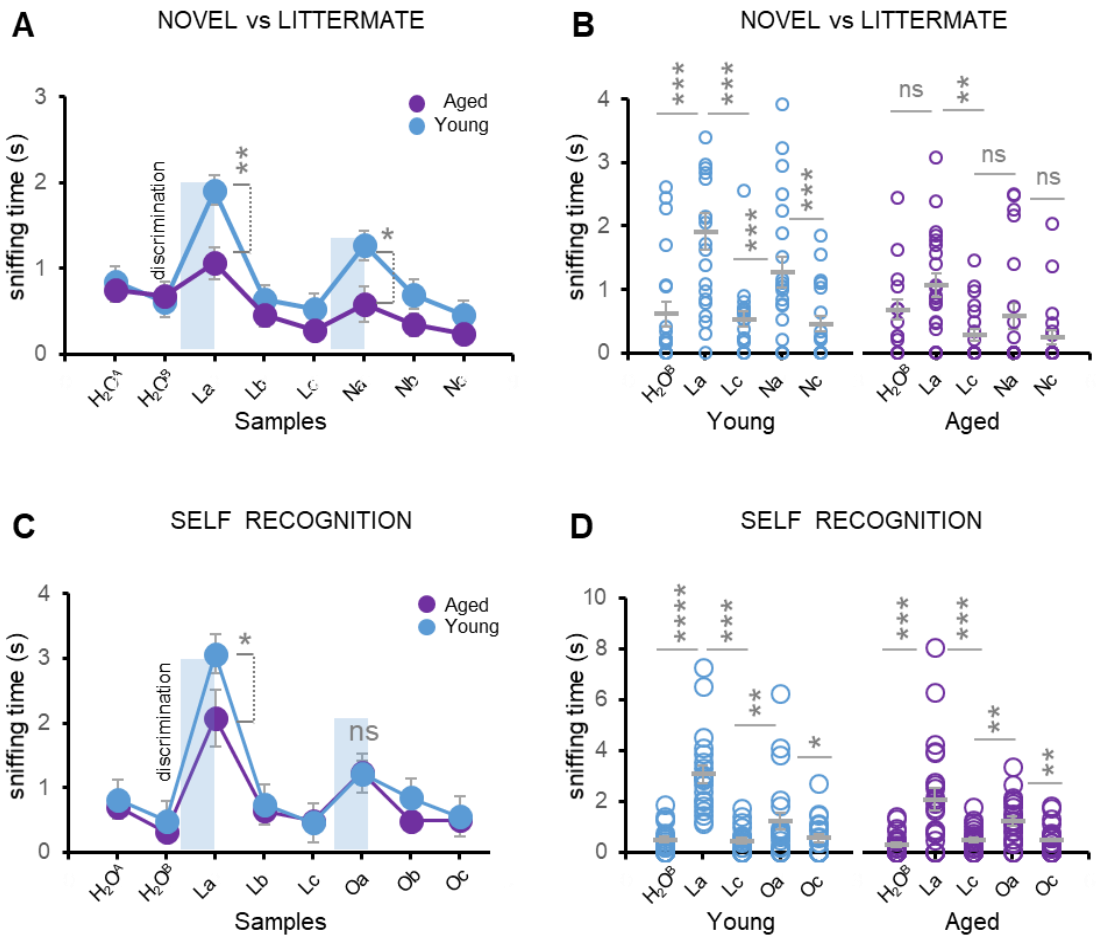

Figure 6. Age-related deficits in social discrimination and habituation are not influenced by previous experience. A) Average sniffing time of social habituation-dishabituation test in response to odors from novel (N) or littermate (L) subjects. **B)** Dispersion plot of the exploration time of aged and young animals in response to novel or littermate urine samples. **C)** Average sniffing time of social habituation-dishabituation test in response to littermate and the animal´s own urine (O). **D)** Dispersion plot of exploration time of aged and young animals in response to their own´s or littermate urine samples. Thick lines in dispersion plots indicate mean ± SEM. Number of mice: young: n = 21; aged: n = 23. Data were analyzed by a one-way ANOVA with Tukey´s test to test multiple comparisons with more than one variable. * P ≤ 0.05; ** P ≤ 0.01; *** P ≤ 0.001; **** P ≤ 0.0001.

FIGURE 7

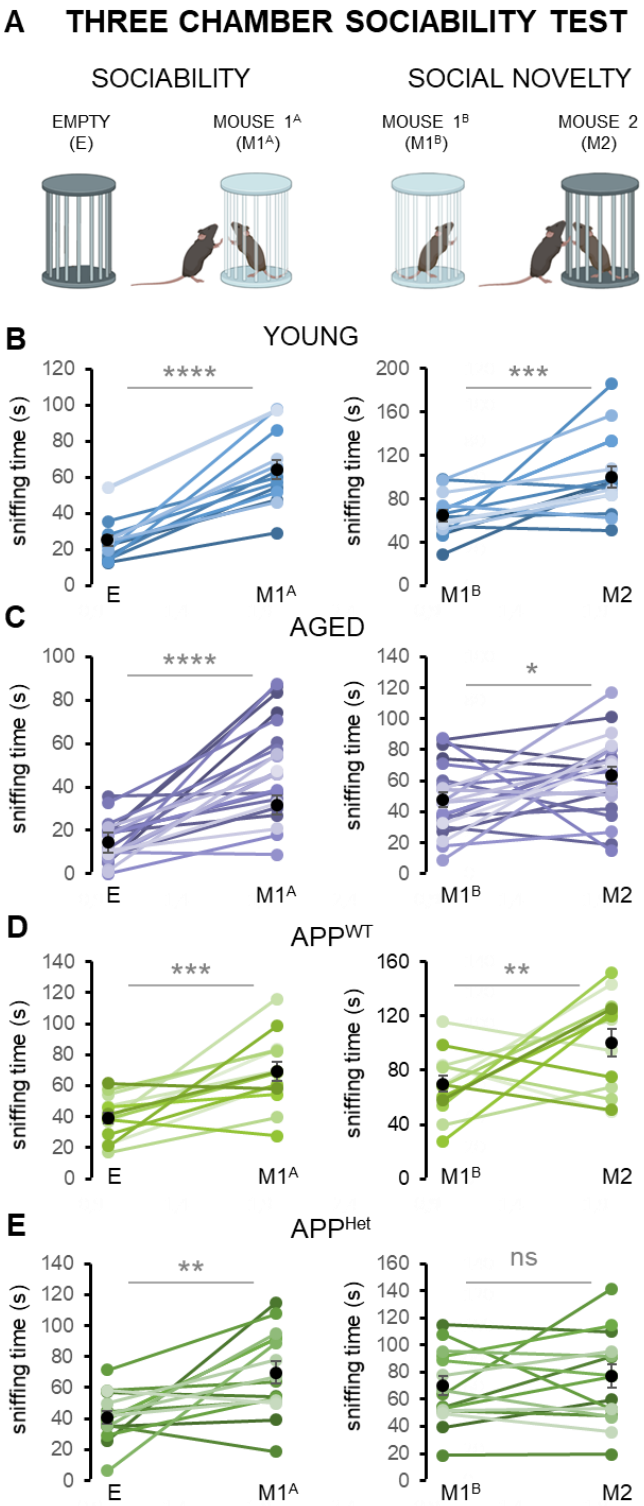

Figure 7. Social novelty is disrupted during pathological aging. A) Schematics of the three chamber test used in this study to test sociability and social novelty. In the sociability phase the sniffing time of E and $M1^A$ are compared. Social novelty is estimated by quantifying the sniffing time of exploring $M1^B$ versus M2. **B)** Dispersion plots of the sniffing times of E-$M1^A$ (sociability) and $M1^B$-M2 (social novelty) for young wild type mice. **C)** Dispersion plots of the sniffing times of E-M1A (sociability) and $M1^B$-M2 (social novelty) for aged wild type mice. D) Dispersion plots of the sniffing times of E-$M1^A$ (sociability) and $M1^B$-M2 (social novelty) for middle age APPWT mice. E) Dispersion plots of the sniffing times of E-$M1^A$ (sociability) and $M1^B$-M2 (social novelty) for middle age APP^{Het} mice. Black dots in the paired plots indicate mean ± SEM. Number of mice: young: n = 10; aged: n = 14; middle age control: n = 10; middle age $APP/PS1^{Het}$: n = 12. Data were analyzed by a one-way ANOVA with Tukey´s test to test multiple comparisons with more than one variable. * $P \leq 0.05$; ** $P \leq 0.01$; *** $P \leq 0.001$; **** $P \leq 0.0001$.

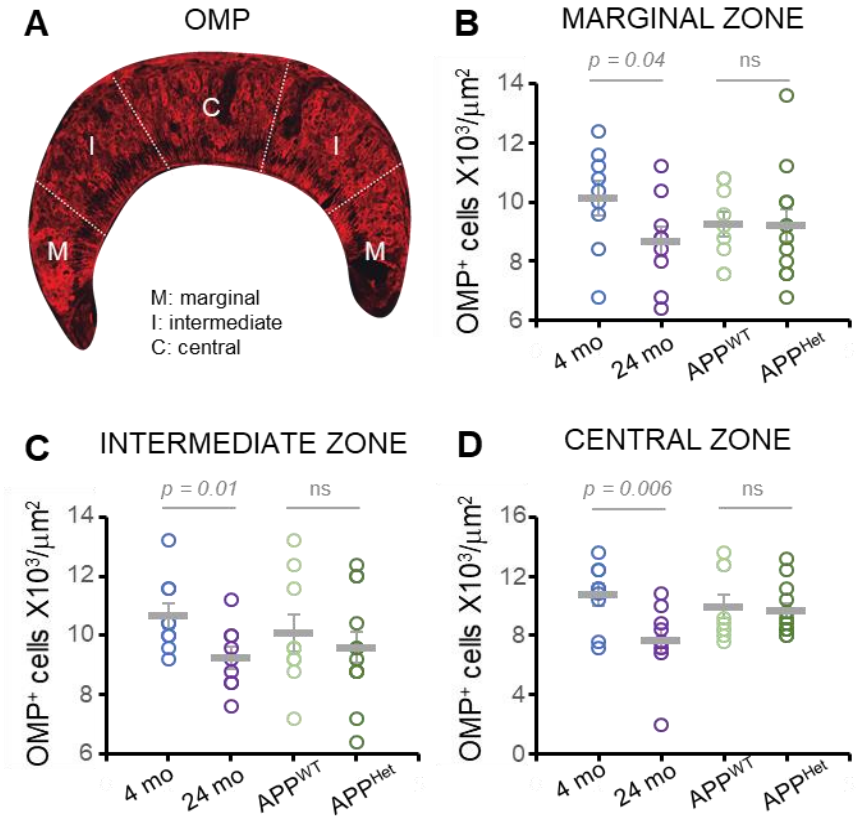

Supplementary Figure 1 (related to Figure 1). Structural modifications of the mouse VSE and AOB during natural and pathological aging. A) Schematics depicting the VNO divisions into marginal (M), intermediate (I) and central (C). **B-D)** Dispersion plots of the number of OMP$^+$ cells in the marginal, intermediate and central zone of the VSE. Thick lines in the dispersion plots indicate mean ± SEM. Data were obtained from 10-16 slices from at least three animals per condition. Statistical comparisons were calculated by one-way ANOVA with Tukey´s test for multiple comparisons with a single variable. P value < 0.05 is considered significant. P values are indicated in the plot.

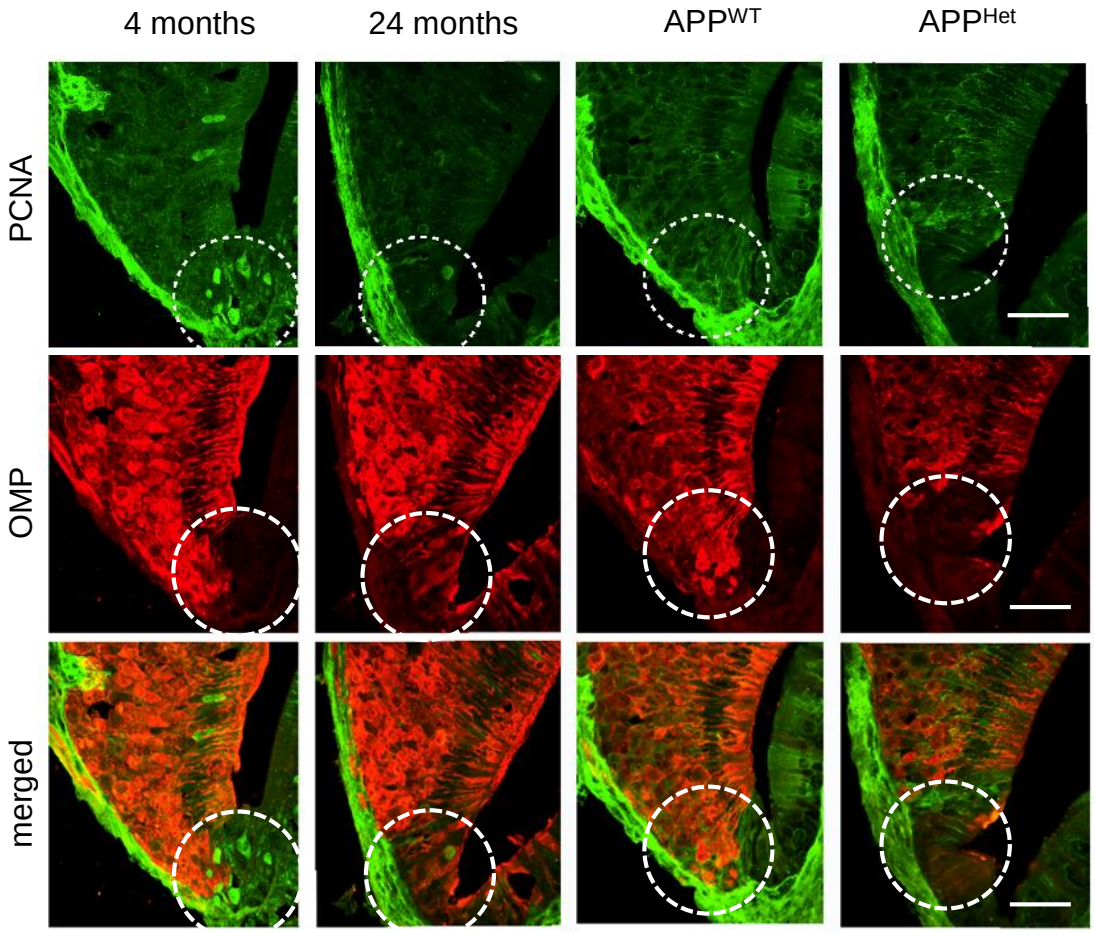

Supplementary Figure 2 (related to Figure 2). The proliferative niche of the VSE is reduced during natural, but not pathological aging. Representative confocal images of both OMP and PCNA staining in the VSE proliferative niche. To note there is no overlapping signal between the two markers indicating the identification of cells at different maturation stages. Circles indicate the proliferative marginal region of the VSE. Scale bar represents 20 μm. Data were obtained from ten slices from animal of each condition.

SOCIAL ODOR EXPLORATION – NATURAL AGING

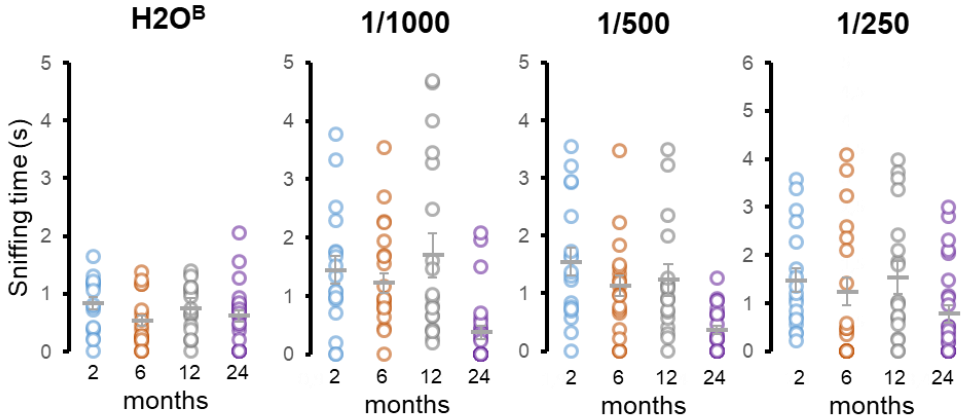

H2O^B	
Comparison	***P***
2 m vs 6 m	**0.02**
2 m vs 12 m	ns
2 m vs 24 m	ns
6 m vs 12 m	ns
6 m vs 24 m	ns
12 m vs 24 m	ns

1:1000 urine dilution	
Comparison	***P***
2 m vs 6 m	ns
2 m vs 12 m	ns
2 m vs 24 m	**0.0007**
6 m vs 12 m	ns
6 m vs 24 m	**0.0004**
12 m vs 24 m	**0.002**

1:500 urine dilution	
Comparison	***P***
2 m vs 6 m	ns
2 m vs 12 m	ns
2 m vs 24 m	**0.0002**
6 m vs 12 m	ns
6 m vs 24 m	**0.0005**
12 m vs 24 m	**0.0008**

1:250 urine dilution	
Comparison	***P***
2 m vs 6 m	ns
2 m vs 12 m	ns
2 m vs 24 m	**0.03**
6 m vs 12 m	ns
6 m vs 24 m	ns
12 m vs 24 m	**0.04**

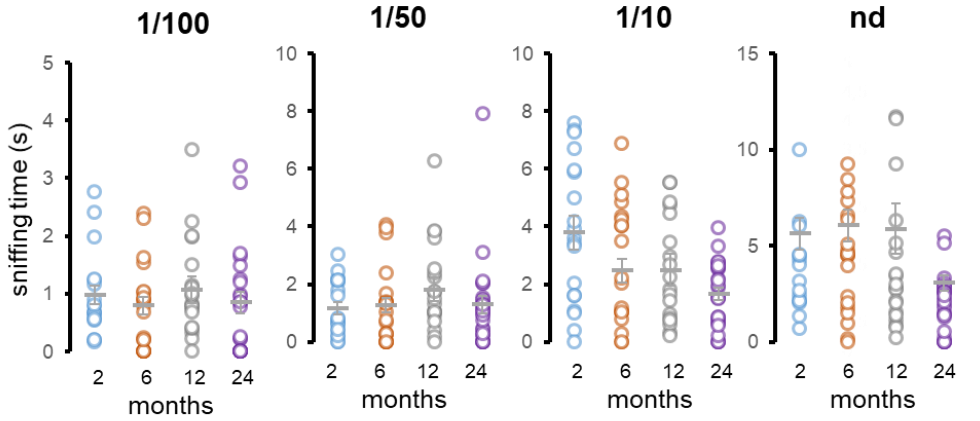

1:100 urine dilution	
Comparison	***P***
2 m vs 6 m	ns
2 m vs 12 m	ns
2 m vs 24 m	ns
6 m vs 12 m	ns
6 m vs 24 m	ns
12 m vs 24 m	ns

1:50 urine dilution	
Comparison	***P***
2 m vs 6 m	ns
2 m vs 12 m	ns
2 m vs 24 m	ns
6 m vs 12 m	ns
6 m vs 24 m	ns
12 m vs 24 m	ns

1:10 urine dilution	
Comparison	***P***
2 m vs 6 m	**0.08**
2 m vs 12 m	**0.04**
2 m vs 24 m	**0.002**
6 m vs 12 m	ns
6 m vs 24 m	ns
12 m vs 24 m	ns

Non diluted	
Comparison	***P***
2 m vs 6 m	ns
2 m vs 12 m	ns
2 m vs 24 m	**0.04**
6 m vs 12 m	ns
6 m vs 24 m	**0.003**
12 m vs 24 m	**0.02**

dilution / age	*H_2O^B*	*1:000*	*1:500*	*1:250*	*1.100*	*1:50*	*1:10*	*nd*
	n	**n**	***n***	***n***	***n***	***n***	***n***	***n***
2 months	18	18	18	18	18	19	19	15
6 months	24	19	20	20	19	21	20	21
12 months	20	19	20	19	20	20	18	19
24 months	26	25	25	25	26	27	26	26

Supplementary Figure 3 (related to Figure 3). Statistical comparison of the exploration time between different ages for each dilution. Dispersion plots represent the sniffing time of 2, 6, 12 and 24 months-old animals for the various serial dilutions tested in **Figure 3**. Thick grey lines indicate mean ± SEM. Number of mice for each condition and the P values for each statistical comparison is indicated in the tables below. Data were analyzed by a one-way ANOVA with Tukey´s test to test multiple comparisons with more than one variable.

SOCIAL ODOR EXPLORATION – NATURAL AGING

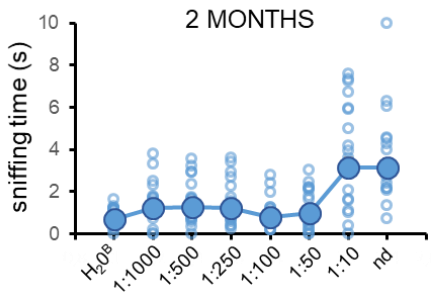

One Way ANOVA – Tukey test

2 months	
Comparison	***P***
H_2O^B vs 1/1000	0.91
H_2O^B vs 1/500	0.81
1/1000 vs 1/500	1.00
H_2O^B vs 1/250	0.88
1/250 vs 1/1000	1.00
1/250 vs 1/500	1.00
H_2O^B vs 1/100	0.99
1/100 vs 1/1000	0.97
1/100 vs 1/500	0.93
1/100 vs 1/250	0.99
H_2O^B vs 1/50	0.99
1/50 vs 1/1000	0.99
1/500 vs 1/50	0.99
1/250 vs 1/50	0.99

2 months	
Comparison	***P***
1/100 vs 1/50	0.99
H_2O^B vs 1/10	1.5×10^{-7}
1/10 vs 1/1000	5.0×10^{-5}
1/10 vs 1/500	1.3×10^{-4}
1/10 vs 1/250	7.0×10^{-5}
1/10 vs 1/100	5.8×10^{-7}
1/10 vs 1/50	3.0×10^{-4}
Nd vs H_2O^B	1.0×10^{-6}
Nd vs 1/1000	2.2×10^{-4}
Nd vs 1/500	5.2×10^{-4}
Nd vs 1/250	3.0×10^{-4}
Nd vs 1/100	4.0×10^{-6}
Nd vs 1/50	1.8×10^{-5}
Nd vs 1/10	1.00

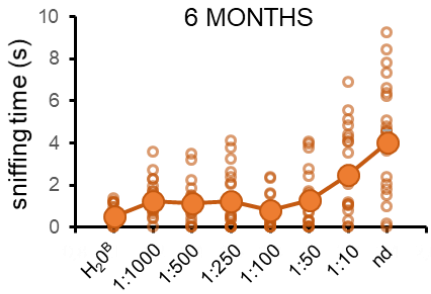

One Way ANOVA – Tukey test

6 months	
Comparison	***P***
H_2O^B vs 1/1000	0.63
H_2O^B vs 1/500	0.85
1/1000 vs 1/500	0.99
H_2O^B vs 1/250	0.82
1/250 vs 1/1000	0.99
1/250 vs 1/500	1.00
H_2O^B vs 1/100	0.99
1/100 vs 1/1000	0.94
1/100 vs 1/500	0.99
1/100 vs 1/250	0.98
H_2O^B vs 1/50	0.53
1/50 vs 1/1000	1.0
1/500 vs 1/50	0.99
1/250 vs 1/50	0.99

6 months	
Comparison	***P***
1/100 vs 1/50	0.90
H_2O^B vs 1/10	6.4×10^{-5}
1/10 vs 1/1000	0.07
1/10 vs 1/500	0.02
1/10 vs 1/250	0.03
1/10 vs 1/100	0.0016
1/10 vs 1/50	0.07
Nd vs H_2O^B	2.2×10^{-8}
Nd vs 1/1000	8.3×10^{-8}
Nd vs 1/500	4.1×10^{-8}
Nd vs 1/250	$4{,}3 \times 10^{-8}$
Nd vs 1/100	4.5×10^{-8}
Nd vs 1/50	7.0×10^{-8}
Nd vs 1/10	0.01

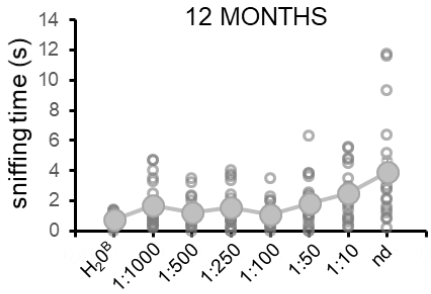

One Way ANOVA – Tukey test

12 months	
Comparison	***P***
H_2O^B vs 1/1000	0.67
H_2O^B vs 1/500	0.98
1/1000 vs 1/500	0.99
H_2O^B vs 1/250	0.85
1/250 vs 1/1000	0.99
1/250 vs 1/500	0.99
H_2O^B vs 1/100	0.99
1/100 vs 1/1000	0.94
1/100 vs 1/500	0.99
1/100 vs 1/250	0.99
H_2O^B vs 1/50	0.50
1/50 vs 1/1000	1.0
1/500 vs 1/50	0.95
1/250 vs 1/50	0.99

12 months	
Comparison	***P***
1/100 vs 1/50	0.85
H_2O^B vs 1/10	0.04
1/10 vs 1/1000	0.84
1/10 vs 1/500	0.31
1/10 vs 1/250	0.67
1/10 vs 1/100	0.17
1/10 vs 1/50	0.92
Nd vs H_2O^B	1.3×10^{-6}
Nd vs 1/1000	0.002
Nd vs 1/500	7.2×10^{-5}
Nd vs 1/250	8.0×10^{-4}
Nd vs 1/100	2.0×10^{-5}
Nd vs 1/50	0.005
Nd vs 1/10	0.20

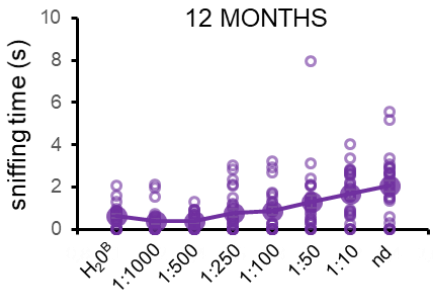

One Way ANOVA – Tukey test

24 months	
Comparison	***P***
H_2O^B vs 1/1000	0.99
H_2O^B vs 1/500	0.98
1/1000 vs 1/500	1.0
H_2O^B vs 1/250	0.99
1/250 vs 1/1000	0.87
1/250 vs 1/500	0.84
H_2O^B vs 1/100	0.99
1/100 vs 1/1000	0.73
1/100 vs 1/500	0.69
1/100 vs 1/250	1.0
H_2O^B vs 1/50	0.25
1/50 vs 1/1000	0.03
1/500 vs 1/50	0.03
1/250 vs 1/50	0.6

24 months	
Comparison	***P***
1/100 vs 1/50	0.76
H_2O^B vs 1/10	0.007
1/10 vs 1/1000	3.4×10^{-4}
1/10 vs 1/500	2.6×10^{-4}
1/10 vs 1/250	0.04
1/10 vs 1/100	0.08
1/10 vs 1/50	0.88
Nd vs H_2O^B	3.4×10^{-5}
Nd vs 1/1000	8.4×10^{-7}
Nd vs 1/500	6.3×10^{-7}
Nd vs 1/250	$4{,}6 \times 10^{-4}$
Nd vs 1/100	0.001
Nd vs 1/50	0.14
Nd vs 1/10	0.89

Supplementary Figure 4 (related to Figure 3). Statistical comparison of exploration time between different dilutions for each analyzed age. Dispersion plots represent the sniffing time and trend curves of 2, 6, 12 and 24 months-old animals for the various serial dilutions tested in **Figure 3**. Thick dots indicate mean ± SEM. P values for each statistical comparison is indicated in the tables on the right. Data were analyzed by a one-way ANOVA with Tukey´s test to test multiple comparisons with more than one variable.

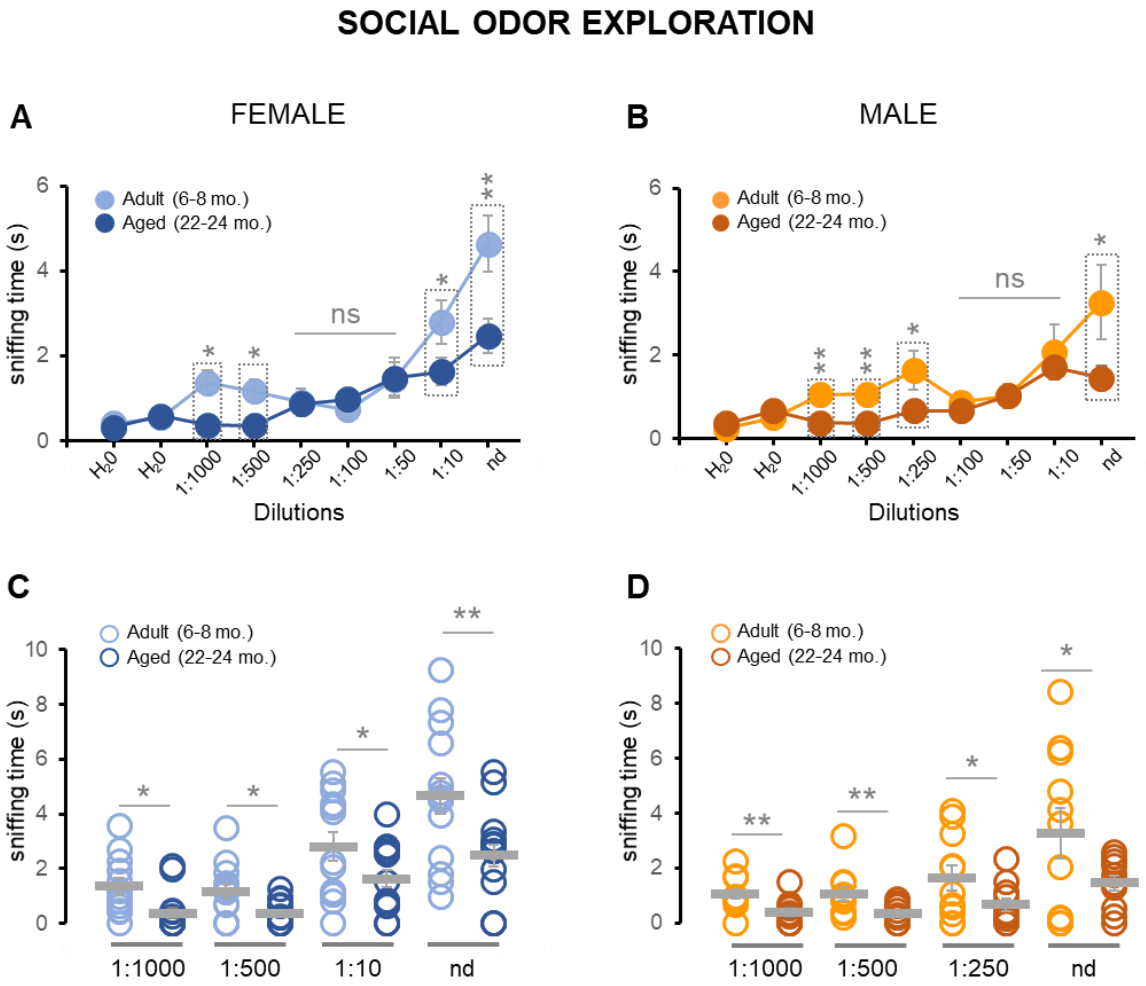

Supplementary Figure 5 (related to Figure 3). Aged-related deficits in social odor exploration exhibit no significant sex differences. A) Average exploration (sniffing) time of urine serial dilutions of adult and aged female wild type mice. **B)** Average exploration (sniffing) time of urine serial dilutions of adult and aged male wild type mice. **C)** Dispersion plots of the sniffing time of urine dilutions that show significant impairments in female mice (nd, non-diluted; 1:10; 1:500; 1:1000). **D)** Dispersion plots of the sniffing time of the urine dilutions that show significant changes in male mice (nd, non-diluted; 1:250; 1:500; 1:1000). Plots indicate mean ± SEM. Number of mice: adult females: n = 13; adult males: n = 11; aged females: n = 14; aged males: n = 11. Data were analyzed by a one-way ANOVA with Tukey´s test to test multiple comparisons with more than one variable. * P ≤ 0.05; ** P ≤ 0.01; *** P ≤ 0.001.

SOCIAL ODOR EXPLORATION - PATHOLOGICAL AGING

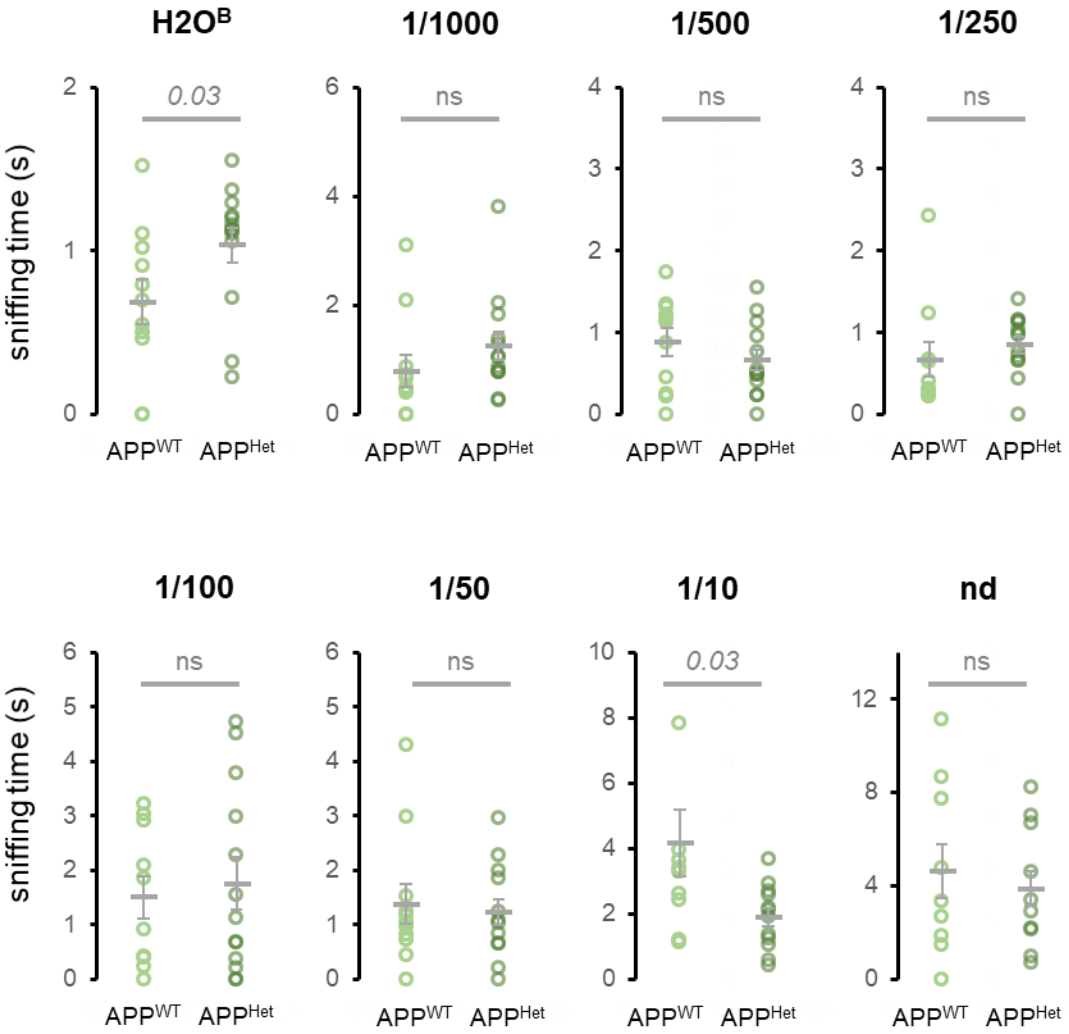

genotype \ dilution	H_2O_B	1:1000	1:500	1:250	1.100	1:50	1:10	nd
	n	*n*	*n*	*n*	*n*	*n*	*n*	*n*
APP^{WT}	11	11	11	10	10	11	10	9
APP^{Het}	13	13	13	13	13	12	12	10

Supplementary Figure 6 (related to Figure 3). Statistical comparison of the exploration time between $APP/PS1^{WT}$ and $APP/PS1^{Het}$ for each dilution. Dispersion plots represent the sniffing time middle age of APP^{WT} and APP^{Het} mice for the various serial dilutions tested in **Figure 3**. Thick grey lines indicate mean ± SEM. Number of mice for each condition and the P values for each statistical comparison is indicated in the tables below. Data were analyzed by a one-way ANOVA with Tukey´s test to test multiple comparisons with more than one variable.

SOCIAL ODOR EXPLORATION – PATHOLOGICAL AGING

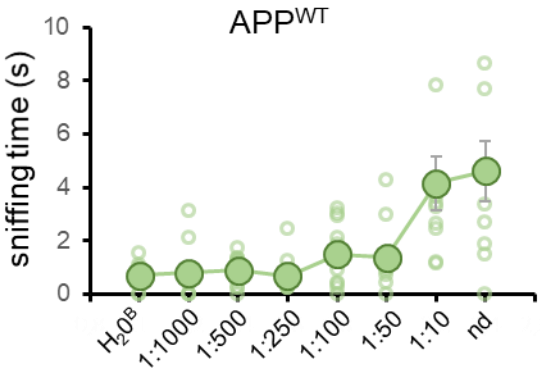

One Way ANOVA – Tukey test

APPWT	
Comparison	***P***
H_2O^B vs 1/1000	1.00
H_2O^B vs 1/500	1.00
1/1000 vs 1/500	1.00
H_2O^B vs 1/250	1.00
1/250 vs 1/1000	1.00
1/250 vs 1/500	0.99
H_2O^B vs 1/100	0.97
1/100 vs 1/1000	0.99
1/100 vs 1/500	0.99
1/100 vs 1/250	0.97
H_2O^B vs 1/50	0.98
1/50 vs 1/1000	0.99
1/500 vs 1/50	0.99
1/250 vs 1/50	0.98

APPWT	
Comparison	***P***
1/100 vs 1/50	1.00
H_2O^B vs 1/10	0.001
1/10 vs 1/1000	0.002
1/10 vs 1/500	0.003
1/10 vs 1/250	0.002
1/10 vs 1/100	0.04
1/10 vs 1/50	0.02
Nd vs H_2O^B	3.1×10^{-4}
Nd vs 1/1000	5.0×10^{-4}
Nd vs 1/500	7.2×10^{-4}
Nd vs 1/250	4.1×10^{-4}
Nd vs 1/100	0.01
Nd vs 1/50	0.005
Nd vs 1/10	0.99

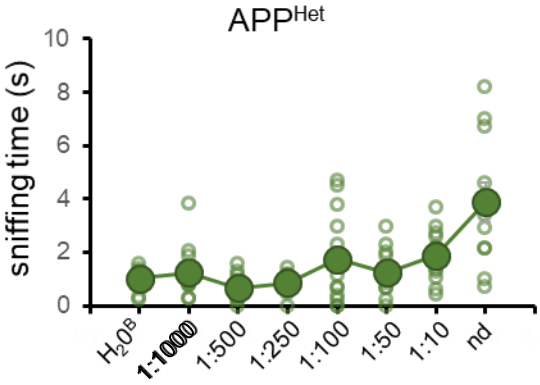

One Way ANOVA – Tukey test

APPHet	
Comparison	***P***
H_2O^B vs 1/1000	0.99
H_2O^B vs 1/500	0.99
1/1000 vs 1/500	0.91
H_2O^B vs 1/250	0.99
1/250 vs 1/1000	0.99
1/250 vs 1/500	0.99
H_2O^B vs 1/100	0.79
1/100 vs 1/1000	0.96
1/100 vs 1/500	0.30
1/100 vs 1/250	0.99
H_2O^B vs 1/50	0.99
1/50 vs 1/1000	1.00
1/500 vs 1/50	0.93
1/250 vs 1/50	0.99

APPHet	
Comparison	***P***
1/100 vs 1/50	0.95
H_2O^B vs 1/10	0.63
1/10 vs 1/1000	0.88
1/10 vs 1/500	0.18
1/10 vs 1/250	0.38
1/10 vs 1/100	0.99
1/10 vs 1/50	0.90
Nd vs H_2O^B	6.6×10^{-6}
Nd vs 1/1000	3.7×10^{-5}
Nd vs 1/500	3.4×10^{-7}
Nd vs 1/250	1.5×10^{-6}
Nd vs 1/100	0.002
Nd vs 1/50	4.7×10^{-5}
Nd vs 1/10	0.005

Supplementary Figure 7 (related to Figure 3). Statistical comparison of the exploration time between different dilutions for APP/PS1^{WT} and APP/PS1^{Het} mice. Dispersion plots represent the sniffing time and trend curves of middle age APP^{WT} and APP^{Het} mice for the various serial dilutions tested in **Figure 3**. Thick dots indicate mean ± SEM. P values for each statistical comparison is indicated in the tables on the right. Data were analyzed by a one-way ANOVA with Tukey´s test to test multiple comparisons with more than one variable.

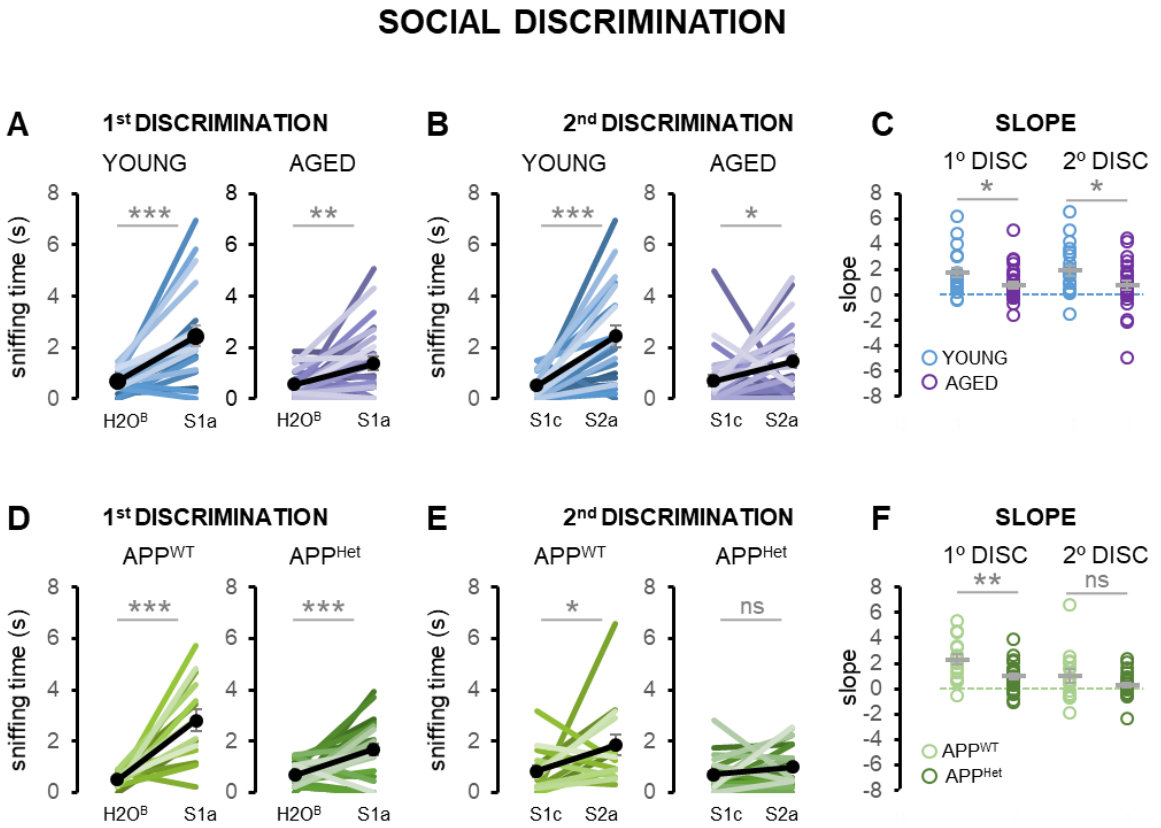

Supplementary Figure 8 (related to Figure 5). Social discrimination is reduced during natural and pathological aging. A) Dispersion plots of the sniffing time of the first discrimination phase (H2O-S1a) for young and aged wild type animals. **B)** Dispersion plots of the sniffing time of the second discrimination phase (S1c-S2a) for young and aged wild type animals. **C)** Dispersion plots of the slope values of the first and second discrimination phases of young and aged mice. **D)** Dispersion plots of the sniffing time of the first discrimination phase (H2O-S1a) for of APP^{WT} and APP^{Het} mice. **E)** Dispersion plots of the sniffing time of the second discrimination phase (S1c-S2a) for of APP^{WT} and APP^{Het} mice. **F)** Dispersion plots of the slope values of the first and second discrimination phases of APP^{WT} and APP^{Het} mice. Black dots in A, B, D, and E and thick lines in C and F indicate mean ± SEM. Data were analyzed by one-way ANOVA with Tukey´s test. * $P \leq 0.05$; ** $P \leq 0.01$; *** $P \leq 0.001$.

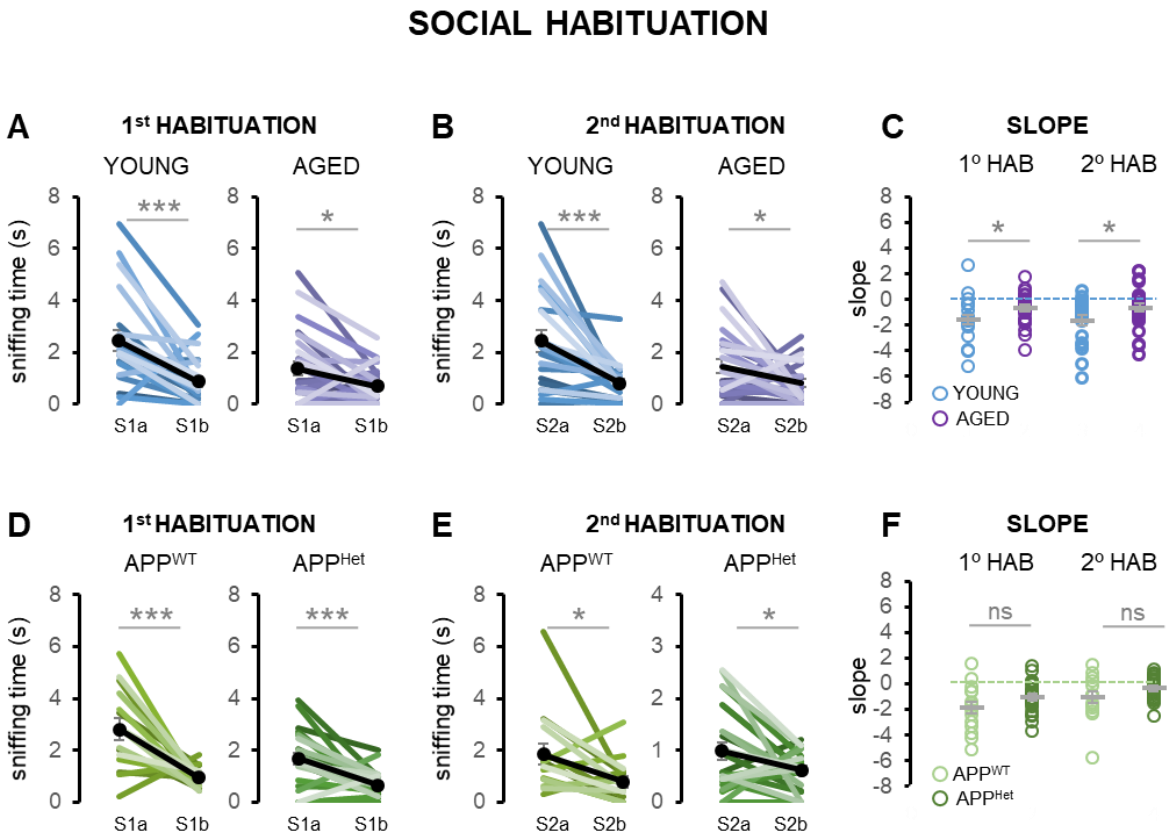

Supplementary Figure 9 (related to Figure 5). Social habituation is diminished during natural and pathological aging. A) Dispersion plots of the sniffing time of the first habituation phase (S1a-S1b) for young and aged wild type animals. **B)** Dispersion plots of the sniffing time of the second habituation phase (S2a-S2b) for young and aged wild type animals. **C)** Dispersion plots of the slope values of the first and second habituation phases of young and aged mice. **D)** Dispersion plots of the sniffing time of the first habituation phase (S1a-S1b) for of APP^{WT} and APP^{Het} mice. **E)** Dispersion plots of the sniffing time of the second habituation phase (S2a-S2b) for of APP^{WT} and APP^{Het} mice. **F)** Dispersion plots of the slope values of the first and second habituation phases of APP^{WT} and APP^{Het} mice. Black dots in **A, B, D**, and **E** and thick lines in **C** and **F** indicate mean ± SEM. Data were analyzed by one-way ANOVA with Tukey´s test. * $P \leq 0.05$; ** $P \leq 0.01$; *** $P \leq 0.001$.

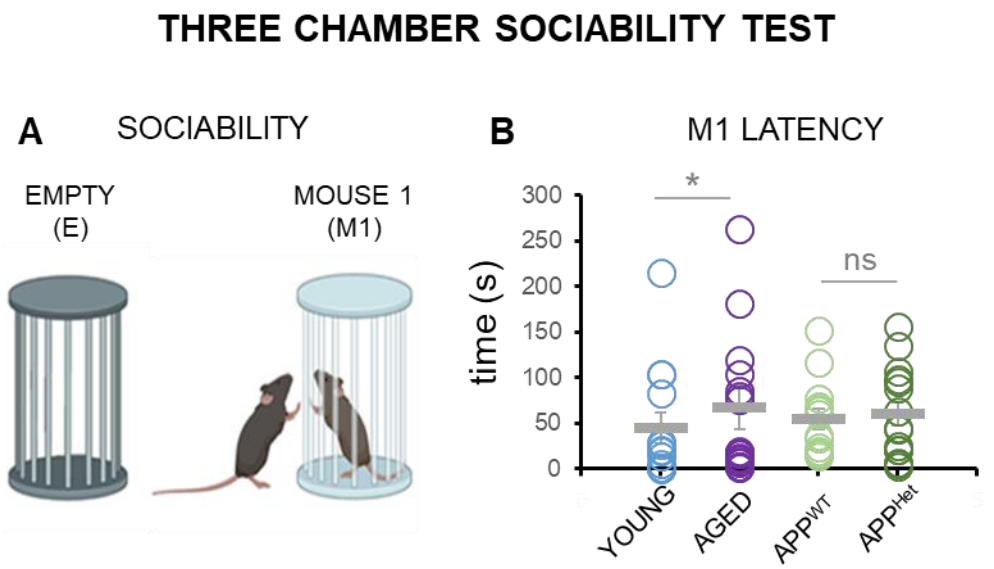

Supplementary Figure 10 (related to Figure 7). Latency to approach the first stranger (M1) in the three chamber sociability test is increased in naturally aged animals. A) The sociability phase of the three chamber test involves exposing the test animal to a stranger mouse (M1) for the first time, which elicits an increase in the exploration time in that side of the chamber. **B)** Dispersion plots of the latency to approach M1 during the first encounter of the sociability phase. Thick lines indicate mean ± SEM. Data were analyzed by one way-ANOVA with Tukey´s test. * $P \leq 0.05$.